# A New Equation of State for H$_2$O Ice Ih

**Rainer Feistel**[a]

*Leibniz-Institut für Ostseeforschung, Universität Rostock, D-18119 Warnemünde, Germany*

**Wolfgang Wagner**

*Lehrstuhl für Thermodynamik, Ruhr-Universität Bochum, D-44780 Bochum, Germany*

Various thermodynamic equilibrium properties of naturally abundant, hexagonal ice (ice Ih) of water (H$_2$O) have been used to develop a Gibbs energy function $g(T,p)$ of temperature and pressure, covering the ranges 0–273.16 K and 0 Pa–210 MPa, expressed in the temperature scale ITS-90. It serves as a fundamental equation from which additional properties are obtained as partial derivatives by thermodynamic rules. Extending previously developed Gibbs functions, it covers the entire existence region of ice Ih in the $T$-$p$ diagram. Close to zero temperature, it obeys the theoretical cubic limiting law of Debye for heat capacity and Pauling's residual entropy. It is based on a significantly enlarged experimental data set compared to its predecessors. Due to the inherent thermodynamic cross relations, the formulas for particular quantities like density, thermal expansion, or compressibility are thus fully consistent with each other, are more reliable now, and extended in their ranges of validity. In conjunction with the IAPWS-95 formulation for the fluid phases of water, the new chemical potential of ice allows an alternative computation of the melting and sublimation curves, being improved especially near the triple point, and valid down to 130 K sublimation temperature. It provides an absolute entropy reference value for liquid water at the triple point. © *2006 American Institute of Physics.* [DOI: 10.1063/1.2183324]

Key words: compressibility; density; entropy; enthalpy; Gibbs energy; heat capacity; ice; melting point; sublimation pressure; thermal expansion; thermodynamic properties; water.

## Contents

### List of Tables

[a]Electronic mail: rainer.feistel@io-warnemuende.de

http://jpcrd.aip.org/resource/1/jpcrbu/v35/i2/p1021_s1

### List of Figures

## List of Symbols

| Symbol | Physical Quantity | Unit |
|---|---|---|
| $c_p$ | Specific isobaric heat capacity of ice | $\mathrm{J\,kg^{-1}\,K^{-1}}$ |
| $\mathrm{d}p_{\mathrm{melt}}/\mathrm{d}T$ | Clausius–Clapeyron slope of the melting curve | $\mathrm{Pa\,K^{-1}}$ |
| $f$ | Specific Helmholtz energy of ice | $\mathrm{J\,kg^{-1}}$ |
| $g,\ g^{\mathrm{Ih}}$ | Specific Gibbs energy of ice | $\mathrm{J\,kg^{-1}}$ |
| $g^{\mathrm{L}}$ | Specific Gibbs energy of liquid water | $\mathrm{J\,kg^{-1}}$ |
| $g^{\mathrm{V}}$ | Specific Gibbs energy of water vapor | $\mathrm{J\,kg^{-1}}$ |
| $g_0$ | Residual Gibbs energy, Table 4 | $\mathrm{J\,kg^{-1}}$ |
| $g_{00} \cdots g_{04}$ | Real constants, Table 2 | $\mathrm{J\,kg^{-1}}$ |
| $h$ | Specific enthalpy of ice | $\mathrm{J\,kg^{-1}}$ |
| $h^{\mathrm{L}}$ | Specific enthalpy of liquid water | $\mathrm{J\,kg^{-1}}$ |
| $h^{\mathrm{V}}$ | Specific enthalpy of water vapor | $\mathrm{J\,kg^{-1}}$ |
| $k$ | Uncertainty coverage factor | |
| $K_{\mathrm{GC47}}$ | Bunsen calorimeter calibration factor of Ginnings and Coruccini (1947) | $\mathrm{J\,kg^{-1}}$ |
| $M$ | Molar mass of water, $M = 18.015\,268\ \mathrm{g\,mol^{-1}}$ [IAPWS (2005)] | $\mathrm{g\,mol^{-1}}$ |
| $p$ | Pressure | Pa |
| $p_0$ | Normal pressure, $p_0 = 101\,325$ Pa | Pa |
| $p_{\mathrm{subl}}$ | Sublimation pressure | Pa |
| $p_{\mathrm{subl}}^{\mathrm{CC}}$ | Clausius–Clapeyron sublimation pressure | Pa |
| $p_{\mathrm{t}}$ | Triple point pressure, $p_{\mathrm{t}} = 611.657$ Pa | Pa |
| $R$ | Specific gas constant, $R = R_{\mathrm{m}}/M = 461.523\,64\ \mathrm{J\,kg^{-1}\,K^{-1}}$ | $\mathrm{J\,kg^{-1}\,K^{-1}}$ |
| $R_{\mathrm{m}}$ | Molar gas constant, $R_{\mathrm{m}} = 8.314\,472\ \mathrm{J\,mol^{-1}\,K^{-1}}$ [Mohr and Taylor (2005)] | $\mathrm{J\,mol^{-1}\,K^{-1}}$ |
| $r_1$ | Complex constant, Table 2 | $\mathrm{J\,kg^{-1}\,K^{-1}}$ |
| $r_2$ | Complex function, Table 4 | $\mathrm{J\,kg^{-1}\,K^{-1}}$ |
| $r_{20} \cdots r_{22}$ | Complex constants, Table 2 | $\mathrm{J\,kg^{-1}\,K^{-1}}$ |
| $s$ | Specific entropy of ice | $\mathrm{J\,kg^{-1}\,K^{-1}}$ |
| $s^{\mathrm{L}}$ | Specific entropy of liquid water | $\mathrm{J\,kg^{-1}\,K^{-1}}$ |
| $s^{\mathrm{V}}$ | Specific entropy of water vapor | $\mathrm{J\,kg^{-1}\,K^{-1}}$ |
| $s_0$ | Residual entropy, Table 2 | $\mathrm{J\,kg^{-1}\,K^{-1}}$ |
| $T$ | Absolute temperature (ITS-90) | K |
| $T_0$ | Celsius zero point, $T_0 = 273.15$ K | K |

| $T_{\mathrm{melt}}$ | Melting temperature of ice | K |
|---|---|---|
| $T_{\mathrm{melt},p_0}$ | Normal pressure melting point, $T_{\mathrm{melt},p_0}=273.152\,519$ K | K |
| $T_{\mathrm{t}}$ | Triple point temperature, $T_{\mathrm{t}}=273.16$ K | K |
| $t_1$, $t_2$ | Complex constants, Table 2 | |
| $u$ | Specific internal energy of ice | J kg$^{-1}$ |
| $U$ | Expanded uncertainty | |
| $u_{\mathrm{c}}$ | Combined standard uncertainty | |
| $u^{\mathrm{L}}$ | Specific internal energy of liquid water | J kg$^{-1}$ |
| $\nu$ | Specific volume of ice | m$^3$ kg$^{-1}$ |
| $\nu^{\mathrm{L}}$ | Specific volume of liquid water | m$^3$ kg$^{-1}$ |
| $\nu^{\mathrm{V}}$ | Specific volume of water vapor | m$^3$ kg$^{-1}$ |
| $z$ | Any complex number | |
| $\alpha$ | Cubic expansion coefficient of ice | K$^{-1}$ |
| $\beta$ | Pressure coefficient of ice | Pa K$^{-1}$ |
| $\Delta c_p$ | Specific isobaric heat capacity difference | J kg$^{-1}$ K$^{-1}$ |
| $\Delta g$ | Specific Gibbs energy difference | J kg$^{-1}$ |
| $\Delta h$ | Specific enthalpy difference | J kg$^{-1}$ |
| $\Delta h_{\mathrm{melt}}$ | Specific melting enthalpy | J kg$^{-1}$ |
| $\Delta h_{\mathrm{subl}}$ | Specific sublimation enthalpy | J kg$^{-1}$ |
| $\Delta h_{\mathrm{t}}$ | Triple point specific sublimation enthalpy | J kg$^{-1}$ |
| $\Delta p$ | Pressure difference | Pa |
| $\Delta s$ | Specific entropy difference | J kg$^{-1}$ K$^{-1}$ |
| $\Delta s_{\mathrm{melt}}$ | Specific melting entropy | J kg$^{-1}$ K$^{-1}$ |
| $\Delta s_{\mathrm{subl}}$ | Specific sublimation entropy | J kg$^{-1}$ K$^{-1}$ |
| $\Delta T$ | Temperature difference | K |
| $\Delta \nu$ | Specific volume difference | m$^3$ kg$^{-1}$ |
| $\Delta \nu_{\mathrm{melt}}$ | Specific melting volume | m$^3$ kg$^{-1}$ |
| $\Delta \nu_{\mathrm{subl}}$ | Specific sublimation volume | m$^3$ kg$^{-1}$ |
| $\kappa_s$ | Isentropic compressibility of ice | Pa$^{-1}$ |
| $\kappa_T$ | Isothermal compressibility of ice | Pa$^{-1}$ |
| $\mu^{\mathrm{Ih}}$ | Chemical potential of ice | J kg$^{-1}$ |
| $\pi$ | Pi, $\pi=3.141\,592\,65...$ | |
| $\pi$ | Reduced pressure, $\pi=p/p_{\mathrm{t}}$ | |
| $\pi_0$ | Reduced normal pressure, $\pi_0=p_0/p_{\mathrm{t}}$ | |
| $\rho$ | Density of ice | kg m$^{-3}$ |
| $\rho_{\mathrm{Hg}}$ | Density of mercury | kg m$^{-3}$ |
| $\rho^{\mathrm{L}}$ | Density of liquid water | kg m$^{-3}$ |
| $\rho^{\mathrm{V}}$ | Density of water vapor | kg m$^{-3}$ |
| $\tau$ | Reduced temperature, $\tau=T/T_{\mathrm{t}}$ | |
| $\chi$ | Clausius–Clapeyron coefficient | mK MPa$^{-1}$ |

# 1. Introduction

The latest development of more comprehensive and more accurate formula for thermodynamic equilibrium properties of seawater in the form of a Gibbs potential function [Feistel (2003)] was based on the current scientific pure-water standard IAPWS-95 [Wagner and Pruß (2002)]. For an adequately advanced description of freezing points of seawater over the natural, "Neptunian" ranges of salinity and pressure, for the consistent description of sublimation pressures over ice and sea ice, as well as for an improved Gibbs potential formulation of sea ice thermodynamics, the development of a reliable Gibbs function of naturally abundant hexagonal ice Ih was desired, valid over a wide range of pressures and temperatures. The new function constructed

for that purpose is described in this paper. Presented here is its second, corrected version with an extended data base and a modified set of coefficients, but with identical mathematical structure as its predecessor. The detailed derivation of the first version, its mathematical form, and many details of the fitting procedures employed were reported by Feistel and Wagner (2005) in an earlier paper. Both versions differ only within their ranges of uncertainties except for one quantity, the absolute entropy of liquid water, which is only now reproduced within its uncertainty as reported by Cox *et al.* (1989).

After the extensive and systematic laboratory measurements of ice Ih and other solid water phases by Bridgman (1912a, b, 1935, 1937), various reviews on ice properties and comprehensive presentations thereof were published, as e.g., by Pounder (1965), Dorsey (1968), Fletcher (1970), Franks (1972), Hobbs (1974), Wexler (1977), Yen (1981), Hyland and Wexler (1983), Nagornov and Chizhov (1990), Fukusako

(1990), Yen *et al.* (1991), Petrenko (1993), or Petrenko and Whitworth (1999).

The theoretical formalism of classical thermodynamics is, in the strict sense, only valid for equilibrium states. For the case of ice, this means that the thermodynamic potential is designed to describe the ideal structure of a single, undistorted crystal at a state where all possible spontaneous aging processes have passed. These conditions may not always exactly be fulfilled for the experimental data we used. Particularly in the temperature range below 100 K the related theoretical and experimental problems are complicated and still subject to ongoing research. Excessive scatter is observed in measurements of heat capacity and density in the range between 60 and 100 K (see Secs. 3.1. and 3.4.). Results of different works deviate from each other more (up to 0.3% in density) than their particular precisions suggest, so that systematic problems in sample preparations or experimental procedures must be inferred [Dantl and Gregora (1968), Dantl (1967), Dantl (1969), Röttger *et al.* (1994)]. The relaxation to equilibrium is extremely slow between 85 and 100 K [Giauque and Stout (1936)]. A weak density maximum (about 0.1%) was found at 60–70 K by several authors [Jakob and Erk (1929), Dantl (1962), Röttger *et al.* (1994), Tanaka (1998)]. A ferroelectric transition at 100 K was proposed first [Dengel *et al.* (1964), van den Beukel (1968)] but could not be confirmed later [Johari and Jones (1975), Bramwell (1999)]. A phase transition from ice Ih to a perfectly ordered, cubical, denser, and ferroelectric phase XI is supposed to occur between 60 and 100 K [Pitzer and Polissar (1956), Howe and Whitworth (1989), Iedema *et al.* (1998), Petrenko and Whitworth (1999), Kuo *et al.* (2001), Kuo *et al.* (2004), Singer *et al.* (2005)], thus turning ice Ih into a thermodynamically metastable structure below the threshold temperature. Even though a spontaneous transition Ih-XI of pure ice has not been observed experimentally and is unlikely to occur without catalytic acceleration [Pitzer and Polissar (1956), Iedema *et al.* (1998)], partial reconfigurations, proton ordering processes, or frozen-in transient structures may have influenced the results of experiments [Matsuo *et al.* (1986), Yamamuro *et al.* (1987), Johari (1998)].

The Gibbs function derived in this paper ignores the various open questions in the low-temperature region and treats ice Ih like a stable equilibrium phase down to 0 K. This approach is supported by its very good agreement with the entropy difference between 0 K and the normal freezing point (see Sec. 3.5. for details). In consistency with experimental findings of, e.g., Brill and Tippe (1967), it does not exhibit negative thermal expansion coefficients. Adjacent ices II, III, IX, or XI [see e.g. Lobban *et al.* (1998)] are not further considered in the following.

The first proposals to combine ice properties into a Gibbs function were published by Feistel and Hagen (1995), and by Tillner-Roth (1998). Both formulas provide the specific Gibbs energy of ice, $g(T,p)$, in terms of temperature $T$ and pressure $p$, and are based on only restricted data selections from the vicinity of the melting curve. Feistel and Hagen (1995) had used ice properties as summarized by Yen *et al.*
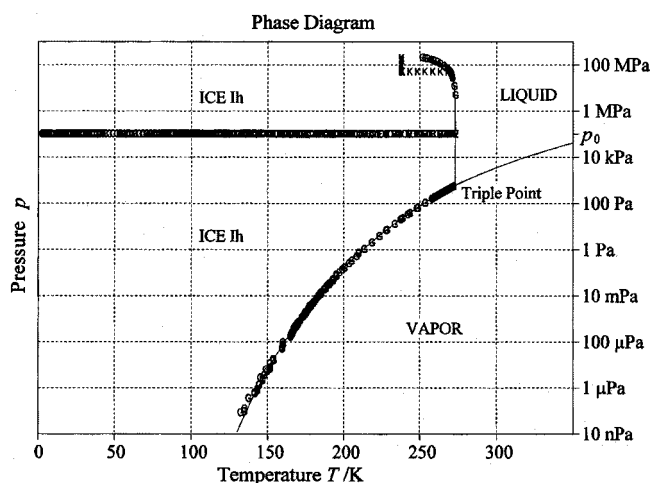


FIG. 1. Phase diagram of liquid water, water vapor, and ice Ih. Adjacent ices II, III, IX, or XI are not considered. Symbols show experimental data points, $C$: specific isobaric heat capacity, $E$: cubic expansion coefficient, $G$: chemical potential, $K$: isentropic compressibility, $V$: density.

(1991), expressed in lowest order polynomials of temperature and pressure near the melting point at normal pressure, later improved by Feistel (2003) for higher pressures using the melting point equation of Wagner *et al.* (1994). Tillner-Roth (1998) used the latter equation together with selected ice properties along the entire melting curve up to the triple point ice I–III–liquid, which is at about 210 MPa and $-22\,°C$ (Fig. 1).

The new formulation presented in this paper improves the previously existing Gibbs functions of ice by additionally including more suitable, theoretical, as well as measured, available ice properties, covering its entire existence region in the temperature-pressure diagram. With very few exceptions, these data are restricted to only three curves in the $T$-$p$ diagram, the sublimation and melting curves, and the normal pressure line (Fig. 1). They have been measured during the past 100 years and are scattered over various publications from cloud physics to geology. No experimental data were available to the authors for the region of high pressures at low temperatures. The new Gibbs potential provides reasonable values for that area, but no uncertainty estimates can be given. All temperature values of the measurements used were converted to the ITS-90 temperature scale. A list of some general constants and values is given in Table 1 for reference.

Attached in parentheses to the given values, estimated combined standard uncertainties $u_c$ are reported [ISO (1993a)], from which by multiplying with the coverage factor $k = 2$ expanded uncertainties $U$ can be obtained, corresponding to a 95% level of confidence. The short notion "uncertainty" used in this paper refers to combined standard uncertainties or to relative combined standard uncertainties, if not stated otherwise.

TABLE 1. Special constants and values used in the paper

| Quantity | Symbol | Value | Unit | Uncertainty | Source |
|---|---|---|---|---|---|
| Triple point pressure | $p_t$ | 611.657 | Pa | 0.010 | Guildner *et al.* (1976) |
| Normal pressure | $p_0$ | 101325 | Pa | exact | ISO (1993b) |
| Triple point temperature | $T_t$ | 273.160 | K | exact | Preston-Thomas (1990) |
| Celsius zero point | $T_0$ | 273.150 | K | exact | Preston-Thomas (1990) |
| Normal melting point | $T_{\text{melt},p_0}$ | 273.152 519 | K | $2 \times 10^{-6}$ | This paper |

## 2. The New Equation of State (Gibbs Potential Function)

The thermodynamic Gibbs potential function $g^{\text{Ih}}(T,p)$ is the specific Gibbs energy of ice Ih, which is equal to the chemical potential $\mu^{\text{Ih}}(T,p)$ of ice, given in mass units. In the following, for simplicity we will generally suppress the superscript "Ih" for ice properties. We express absolute temperature $T$ by a dimensionless variable, the reduced temperature $\tau = T/T_t$ with triple point temperature $T_t$, and absolute pressure $p$ by reduced pressure $\pi = p/p_t$, with triple point pressure $p_t$.

The functional form of $g(T,p)$ for ice Ih is given by Eq. (1) as a function of temperature, with two of its coefficients being polynomials of pressure,

$$g(T,p) = g_0 - s_0 T_t \cdot \tau + T_t \, \text{Re} \sum_{k=1}^{2} r_k \left[ (t_k - \tau) \ln(t_k - \tau) \right.$$

$$\left. + (t_k + \tau) \ln(t_k + \tau) - 2 t_k \ln t_k - \frac{\tau^2}{t_k} \right],$$

$$g_0(p) = \sum_{k=0}^{4} g_{0k} \cdot (\pi - \pi_0)^k, \qquad (1)$$

$$r_2(p) = \sum_{k=0}^{2} r_{2k} \cdot (\pi - \pi_0)^k.$$

The dimensionless normal pressure is $\pi_0 = p_0/p_t$. The real constants $g_{00} - g_{04}$ and $s_0$ as well as the complex constants $t_1$, $r_1$, $t_2$, and $r_{20} - r_{22}$ are given in Table 2. This list of 18 parameters contains two redundant ones which formally ap-

peared during the transformation of six originally real parameters describing heat capacity into four complex numbers [Feistel and Wagner (2005)].

The complex logarithm $\ln(z)$ is meant as the principal value, i.e., it evaluates to imaginary parts in the interval $-\pi < \text{Im}[\ln(z)] \leq +\pi$ (the number Pi, $\pi = 3.1415...$, in this inequality is not to be confused with the symbol of reduced pressure). The complex notation used here has no direct physical reasons but serves for the convenience of analytical partial derivatives and for compactness of the resulting formulas, especially in program code. Complex data types are supported by scientific computer languages like Fortran or C++, thus allowing an immediate implementation of the formulas given, without the need for prior conversion to much more complicated real functions, or for experience in complex calculus.

The residual entropy coefficient $s_0$ is given in Table 2 in the form of two alternative values, its "IAPWS-95" version is required for phase equilibria studies between ice and fluid water in the IAPWS-95 formulation [Wagner and Pruß (2002)], or seawater [Feistel (2003)], while its "absolute" version represents the true physical zero-point entropy of ice [Pauling (1935), Nagle (1966)]:

"IAPWS-95" reference state [Wagner and Pruß (2002)]:

$$u^L(T_t,p_t) = 0 \ \text{J kg}^{-1},$$
$$s^L(T_t,p_t) = 0 \ \text{J kg}^{-1} \text{K}^{-1}, \qquad (2)$$

"Absolute" reference state:

$$g(0,p_0) = -632\,020.233\,449\,497 \ \text{J kg}^{-1},$$
$$s(0,p_0) = 189.13 \ \text{J kg}^{-1} \text{K}^{-1}. \qquad (3)$$

TABLE 2. Coefficients of the Gibbs function as given in Eq. (1)

| Coefficient | Real part | Imaginary part | Unit |
|---|---|---|---|
| $g_{00}$ | $-632\,020.233\,449\,497$ | | J kg$^{-1}$ |
| $g_{01}$ | $0.655\,022\,213\,658\,955$ | | J kg$^{-1}$ |
| $g_{02}$ | $-1.893\,699\,293\,261\,31\text{E}-08$ | | J kg$^{-1}$ |
| $g_{03}$ | $3.397\,461\,232\,710\,53\text{E}-15$ | | J kg$^{-1}$ |
| $g_{04}$ | $-5.564\,648\,690\,589\,91\text{E}-22$ | | J kg$^{-1}$ |
| $s_0$ (absolute) | $189.13$ | | J kg$^{-1}$ K$^{-1}$ |
| $s_0$ (IAPWS-95) | $-3327.337\,564\,921\,68$ | | J kg$^{-1}$ K$^{-1}$ |
| $t_1$ | $3.680\,171\,128\,550\,51\text{E}-02$ | $5.108\,781\,149\,595\,72\text{E}-02$ | |
| $r_1$ | $44.705\,071\,628\,5388$ | $65.687\,684\,746\,3481$ | J kg$^{-1}$ K$^{-1}$ |
| $t_2$ | $0.337\,315\,741\,065\,416$ | $0.335\,449\,415\,919\,309$ | |
| $r_{20}$ | $-72.597\,457\,432\,922$ | $-78.100\,842\,711\,287$ | J kg$^{-1}$ K$^{-1}$ |
| $r_{21}$ | $-5.571\,076\,980\,301\,23\text{E}-05$ | $4.645\,786\,345\,808\,06\text{E}-05$ | J kg$^{-1}$ K$^{-1}$ |
| $r_{22}$ | $2.348\,014\,092\,159\,13\text{E}-11$ | $-2.856\,511\,429\,049\,72\text{E}-11$ | J kg$^{-1}$ K$^{-1}$ |

TABLE 3. Relations of the thermodynamic properties to the equation for the Gibbs energy for ice, Eq. (1), and its derivatives[a]

| Property | Relation | Unit | Eq. |
|---|---|---|---|
| Density $\rho(T,p)=\nu^{-1}=(\partial g/\partial p)_T^{-1}$ | $\rho(T,p)=g_p^{-1}$ | kg m$^{-3}$ | (4) |
| Specific entropy $s(T,p)=-(\partial g/\partial T)_p$ | $s(T,p)=-g_T$ | J kg$^{-1}$ K$^{-1}$ | (5) |
| Specific isobaric heat capacity $c_p(T,p)=T(\partial s/\partial T)_p$ | $c_p(T,p)=-Tg_{TT}$ | J kg$^{-1}$ K$^{-1}$ | (6) |
| Specific enthalpy $h(T,p)=g+Ts$ | $h(T,p)=g-Tg_T$ | J kg$^{-1}$ | (7) |
| Specific internal energy $u(T,p)=g+Ts-p\nu$ | $u(T,p)=g-Tg_T-pg_p$ | J kg$^{-1}$ | (8) |
| Specific Helmholtz energy $f(T,p)=g-p\nu$ | $f(T,p)=g-pg_p$ | J kg$^{-1}$ | (9) |
| Cubic expansion coefficient $\alpha(T,p)=\nu^{-1}(\partial\nu/\partial T)_p$ | $\alpha(T,p)=g_{Tp}/g_p$ | K$^{-1}$ | (10) |
| Pressure coefficient $\beta(T,p)=(\partial p/\partial T)_\nu$ | $\beta(T,p)=-g_{Tp}/g_{pp}$ | Pa K$^{-1}$ | (11) |
| Isothermal compressibility $\kappa_T(T,p)=-\nu^{-1}(\partial\nu/\partial p)_T$ | $\kappa_T(T,p)=-g_{pp}/g_p$ | Pa$^{-1}$ | (12) |
| Isentropic compressibility $\kappa_s(T,p)=-\nu^{-1}(\partial\nu/\partial p)_s$ | $\kappa_s(T,p)=(g_{Tp}^2-g_{TT}g_{pp})/(g_pg_{TT})$ | Pa$^{-1}$ | (13) |

[a]
$$g_T\equiv\left[\frac{\partial g}{\partial T}\right]_p,\quad g_p\equiv\left[\frac{\partial g}{\partial p}\right]_T,\quad g_{TT}\equiv\left[\frac{\partial^2 g}{\partial T^2}\right]_p,\quad g_{Tp}\equiv\left[\frac{\partial^2 g}{\partial T\partial p}\right],\quad g_{pp}\equiv\left[\frac{\partial^2 g}{\partial p^2}\right]_T$$

Superscript L indicates the liquid phase. The property $u$ is the specific internal energy [Eq. (8)]. The theoretical absolute value for the internal energy is given by the relativistic rest energy, a very large number on the order of $10^{17}$ J kg$^{-1}$, which is too impractical to be adopted here. Thus, to conveniently specify $g_{00}$, the second free constant of the reference state defined by Eq. (3), the value of $g$ at zero temperature and normal pressure is chosen here for simplicity to be the same for both reference states.

A collection of the most important relations of the thermodynamic properties to the equation for the Gibbs energy for ice is given in Table 3.

Various properties of ice Ih can be computed by means of partial derivatives of the Gibbs energy. A list of all partial derivatives of $g$ up to second order with respect to the independent variables $p$ and $T$ is given in Table 4.

The Gibbs potential function, Eq. (1), has a compact mathematical structure which is capable of covering the entire range of existence of ice Ih between 0 and 273.16 K and 0 and 211 MPa. It uses 16 free parameters; 14 of them were determined by regression with respect to 522 data points belonging to 32 different groups of measurements (Table 5), the remaining two parameters are subject to the IAPWS-95 definition of internal energy and entropy of liquid water at the triple point, or alternatively, to the physically determined zero point residual entropy, Eqs. (2) or (3). The majority of the measured thermodynamic equilibrium properties are described by the new formulation within their experimental uncertainties (see Table 5). Details on the representation of the experimental data are given in Sec. 3. Additionally, the cubic law of Debye for the heat capacity at low temperatures

as well as the pressure independence of residual entropy are intrinsic properties of the potential function.

## 3. Comparison with Experiments

Of the various experimentally determined ice properties only a representative selection can be discussed here, including density, specific isobaric heat capacity, and cubic expansion coefficient at normal pressure, isentropic compressibility, as well as melting and sublimation pressures. For more details we refer the reader to the paper of Feistel and Wagner (2005).

### 3.1. Density

Specific volume, $\nu$, i.e., the reciprocal of density, $\rho$, is derived from the potential function, Eq. (1), by its pressure derivative, Eq. (4), as given in Table 3. This equation leads to a $T^4$ law for first low-temperature corrections with respect to density at 0 K, in agreement with theory [Landau and Lifschitz (1966)].

The density of ice has practically been determined in very different ways, e.g., by calorimetric [Ginnings and Coruccini (1947)], mechanical [Jacob and Erk (1929)], acoustical [Dantl and Gregora (1968)], optical [Gagnon et al. (1988)], x-ray [Brill and Tippe (1967)] or nuclear methods [Röttger et al. (1994)]. Measurements of different authors often typically deviate from each other by up to about 0.3% (Fig. 2) even though the uncertainty of the particular series claimed by the experimenter may be about 0.04% [Dantl and Gregora (1968)]. A possible cause of this systematic scatter could be

TABLE 4. Equations for the Gibbs energy for ice, Eq. (1), and its derivatives[a]

| Equation for the Gibbs energy $g(T,p)$ and its derivatives[a] | Unit |
|---|---|
| $g(T,p) = g_0 - s_0 T_t \tau + T_t \cdot \text{Re} \left\{ \sum_{k=1}^{2} r_k \left[ (t_k - \tau)\ln(t_k - \tau) + (t_k + \tau)\ln(t_k + \tau) - 2t_k \ln(t_k) - \dfrac{\tau^2}{t_k} \right] \right\}$ <br> with $\tau = T/T_t$, $\pi = p/p_t$, $T_t = 273.16$ K, $p_t = 611.657$ Pa, $g_0(p)$, $r_2(p)$ | J kg$^{-1}$ |
| $g_T = -s_0 + \text{Re} \left\{ \sum_{k=1}^{2} r_k \left[ -\ln(t_k - \tau) + \ln(t_k + \tau) - 2\dfrac{\tau}{t_k} \right] \right\}$ | J kg$^{-1}$ K$^{-1}$ |
| $g_p = g_{0,p} + T_t \, \text{Re} \left\{ r_{2,p} \left[ (t_2 - \tau)\ln(t_2 - \tau) + (t_2 + \tau)\ln(t_2 + \tau) - 2t_2 \ln(t_2) - \dfrac{\tau^2}{t_2} \right] \right\}$ | m$^3$ kg$^{-1}$ |
| $g_{TT} = \dfrac{1}{T_t} \text{Re} \left[ \sum_{k=1}^{2} r_k \left( \dfrac{1}{t_k - \tau} + \dfrac{1}{t_k + \tau} - \dfrac{2}{t_k} \right) \right]$ | J kg$^{-1}$ K$^{-2}$ |
| $g_{Tp} = \text{Re} \left\{ r_{2,p} \left[ -\ln(t_2 - \tau) + \ln(t_2 + \tau) - 2\dfrac{\tau}{t_2} \right] \right\}$ | m$^3$ kg$^{-1}$ K$^{-1}$ |
| $g_{pp} = g_{0,pp} + T_t \, \text{Re} \left\{ r_{2,pp} \left[ (t_2 - \tau)\ln(t_2 - \tau) + (t_2 + \tau)\ln(t_2 + \tau) - 2t_2 \ln(t_2) - \dfrac{\tau^2}{t_2} \right] \right\}$ | m$^3$ kg$^{-1}$ Pa$^{-1}$ |

| $g_0(p)$ equation and its derivatives[b] | Unit | $r_2(p)$ equation and its derivatives[b] | Unit |
|---|---|---|---|
| $g_0(p) = \sum_{k=0}^{4} g_{0k}(\pi - \pi_0)^k$ | J kg$^{-1}$ | $r_2(p) = \sum_{k=0}^{2} r_{2k}(\pi - \pi_0)^k$ | J kg$^{-1}$ K$^{-1}$ |
| with <br> $\pi_0 = \dfrac{p_0}{p_t} = \dfrac{101\ 325\ \text{Pa}}{611.657\ \text{Pa}}$ | | with <br> $\pi_0 = \dfrac{p_0}{p_t} = \dfrac{101\ 325\ \text{Pa}}{611.657\ \text{Pa}}$ | |
| $g_{0,p} = \sum_{k=1}^{4} g_{0k} \dfrac{k}{p_t}(\pi - \pi_0)^{k-1}$ | m$^3$ kg$^{-1}$ | $r_{2,p} = \sum_{k=1}^{2} r_{2k} \dfrac{k}{p_t}(\pi - \pi_0)^{k-1}$ | m$^3$ kg$^{-1}$ K$^{-1}$ |
| $g_{0,pp} = \sum_{k=2}^{4} g_{0k} \dfrac{k(k-1)}{p_t^2}(\pi - \pi_0)^{k-2}$ | m$^3$ kg$^{-1}$ Pa$^{-1}$ | $r_{2,pp} = r_{22} \dfrac{2}{p_t^2}$ | m$^3$ kg$^{-1}$ Pa$^{-1}$ K$^{-1}$ |

[a]
$$g_T \equiv \left[\frac{\partial g}{\partial T}\right]_p, \quad g_p \equiv \left[\frac{\partial g}{\partial p}\right]_T, \quad g_{TT} \equiv \left[\frac{\partial^2 g}{\partial T^2}\right]_p, \quad g_{Tp} \equiv \left[\frac{\partial^2 g}{\partial T \partial p}\right], \quad g_{pp} \equiv \left[\frac{\partial^2 g}{\partial p^2}\right]_T$$

[b]
$$g_{0,p} \equiv \left[\frac{\partial g_0}{\partial p}\right]_T, \quad g_{0,pp} \equiv \left[\frac{\partial^2 g_0}{\partial p^2}\right]_T, \quad r_{2,p} \equiv \left[\frac{\partial r_2}{\partial p}\right]_T, \quad r_{2,pp} \equiv \left[\frac{\partial^2 r_2}{\partial p^2}\right]_T$$

the density lowering effect of aging on ice crystals, which is of the same order of magnitude, another could be the very slow relaxation to equilibrium as observed by Giauque and Stout (1936). The densities 916.71(05) kg m$^{-3}$ of Ginnings and Corruccini (1947) and 916.80(04) kg m$^{-3}$ of Dantl and Gregora (1968) are considered the most accurate determinations at normal pressure and 0 °C. The density maxima found by Jacob and Erk (1929), Dantl (1962), and Röttger *et al.* (1994) are located in the range of enhanced uncertainty between 60 and 90 K (Fig. 2), close to 72 K where a phase transition of ice Ih to the higher ordered ice XI is supposed to occur [Howe and Whitworth (1989), Petrenko and Whitworth (1999)].

## 3.2. Cubic Expansion Coefficient

The cubic expansion coefficient, $\alpha$, is obtained from specific volume and its temperature derivative, Eq. (10), as given in Table 3. At very low temperatures, $\alpha(T)$ follows a cubic law like heat capacity, thus obeying Grüneisen's theo-

retically confirmed $T^3$ law in this limit. Several experiments have shown that linear thermal expansion of ice is isotropic in very good approximation.

Experimental data for $\alpha$ are often derived from the relative change of lattice parameters, and they scatter significantly (Fig. 3). Several findings like those of Jakob and Erk (1929) are apparently not consistent with the Grüneisen limiting law, which predicts vanishing thermal expansion at 0 K with cubic first deviations. The similar results obtained by Röttger *et al.* (1994) are computed here at the temperatures of their measurements from their density polynomial $\rho(T)$ with new coefficients [$A_0 = 128.2147$, $A_1 = 0$, $A_2 = 0$, $A_3 = -1.3152$E$-6$, $A_4 = 2.4837$E$-8$, $A_5 = -1.6064$E$-10$, $A_6 = 4.6097$E$-13$, $A_7 = -4.9661$E$-16$ (W. F. Kuhs, private communication)], improved with respect to the published ones. Although their polynomial for the cubic expansion coefficient is correctly constrained to approach zero at 0 K, its leading quadratic term is not consistent with the required cubic limiting law. Data like those of Lonsdale (1958) are evidently erratic. The very accurate data set of Butkovich (1957) with

TABLE 5. Summary of data used for the determination of the Gibbs function coefficients

| Quantity | Source[a] | $T$ (K) | $p$ (MPa) | No. of data | Required[b] rms | Resulting[c] rms |
|---|---|---|---|---|---|---|
| $g$ | B12 | 251–273 | 10–210 | 15 | 1113 J kg$^{-1}$ | 222 J kg$^{-1}$ |
| $g$ | HS87 | 259–273 | 5–147 | 6 | 500 J kg$^{-1}$ | 48 J kg$^{-1}$ |
| $g$ | JPH70 | 257–273 | 0.0001–0.0006 | 45 | 139 J kg$^{-1}$ | 132 J kg$^{-1}$ |
| $g$ | DO65 | 257–273 | 0.0001–0.0006 | 6 | 86 J kg$^{-1}$ | 175 J kg$^{-1}$ |
| $dp_{melt}/dT$ | GC47 | 273 | 0.1 | 1 | 3 kPa K$^{-1}$ | 1.4 kPa K$^{-1}$ |
| $dp_{melt}/dT$ | D05 | 273 | 0.1 | 1 | 7 kPa K$^{-1}$ | 4.6 kPa K$^{-1}$ |
| $dp_{melt}/dT$ | G13 | 273 | 0.1 | 1 | 11 kPa K$^{-1}$ | 10.8 kPa K$^{-1}$ |
| $s$ | GS36 | 273 | 0.1 | 1 | 0.8 J kg$^{-1}$ K$^{-1}$ | 0.17 J kg$^{-1}$ K$^{-1}$ |
| $s$ | O39 | 273 | 0.1 | 1 | 0.7 J kg$^{-1}$ K$^{-1}$ | 0.39 J kg$^{-1}$ K$^{-1}$ |
| $s$ | HMSS74 | 273 | 0.1 | 1 | 0.7 J kg$^{-1}$ K$^{-1}$ | 0.05 J kg$^{-1}$ K$^{-1}$ |
| $s$ | CWM89 | 298 | 0.1 | 1 | 1.7 J kg$^{-1}$ K$^{-1}$ | 0.8 J kg$^{-1}$ K$^{-1}$ |
| $c_p$ | GS36 | 16–268 | 0.1 | 61 | relative 2% | relative 0.88% |
| $c_p$ | FLM60 | 2–27 | 0.1 | 59 | relative 2% | relative 3.0% |
| $c_p$ | HMSS74 | 13–268 | 0.1 | 160 | relative 2% | relative 0.6% |
| $\nu$ | LP60 | 93–263 | 0.1 | 10 | 1 cm$^3$ kg$^{-1}$ | 0.91 cm$^3$ kg$^{-1}$ |
| $\nu$ | BT67 | 13–193 | 0.1 | 10 | 0.3 cm$^3$ kg$^{-1}$ | 0.52 cm$^3$ kg$^{-1}$ |
| $\nu$ | M34 | 273 | 0.1 | 1 | 0.84 cm$^3$ kg$^{-1}$ | 0.29 cm$^3$ kg$^{-1}$ |
| $\nu$ | T55 | 227 | 0.1 | 1 | 0.37 cm$^3$ kg$^{-1}$ | 1.1 cm$^3$ kg$^{-1}$ |
| $\nu$ | B55 | 268–270 | 0.1 | 28 | 0.2 cm$^3$ kg$^{-1}$ | 0.12 cm$^3$ kg$^{-1}$ |
| $\nu$ | DG68 | 273 | 0.1 | 1 | 0.04 cm$^3$ kg$^{-1}$ | 0.093 cm$^3$ kg$^{-1}$ |
| $\nu$ | JE29 | 20–273 | 0.1 | 34 | 0.5 cm$^3$ kg$^{-1}$ | 0.57 cm$^3$ kg$^{-1}$ |
| $\nu$ | REIDK94 | 17–265 | 0.1 | 19 | 1 cm$^3$ kg$^{-1}$ | 0.34 cm$^3$ kg$^{-1}$ |
| $\nu$ | B35 | 251–273 | 0.1–211 | 6 | 10 cm$^3$ kg$^{-1}$ | 12 cm$^3$ kg$^{-1}$ |
| $\nu$ | GKCW88 | 238 | 0.1–201 | 5 | 1 cm$^3$ kg$^{-1}$ | 1.4 cm$^3$ kg$^{-1}$ |
| $(\partial\nu/\partial T)_p$ | B57 | 243–273 | 0.1 | 7 | 2 mm$^3$ kg$^{-1}$ K$^{-1}$ | 1.9 mm$^3$ kg$^{-1}$ K$^{-1}$ |
| $\kappa_s$ | D67 | 133–273 | 0.1 | 15 | 4 TPa$^{-1}$ | 3.4 TPa$^{-1}$ |
| $\kappa_s$ | P66 | 60–110 | 0.1 | 6 | 1 TPa$^{-1}$ | 0.46 TPa$^{-1}$ |
| $\kappa_s$ | BR69 | 253 | 0.1 | 1 | 8 TPa$^{-1}$ | 6.5 TPa$^{-1}$ |
| $\kappa_s$ | GKC80 | 257–270 | 0.1 | 3 | 0.7 TPa$^{-1}$ | 1.1 TPa$^{-1}$ |
| $\kappa_s$ | GKCW88 | 238–268 | 0.1 | 7 | 0.7 TPa$^{-1}$ | 0.57 TPa$^{-1}$ |
| $\kappa_s$ | GKCW88 | 238 | 0.1–201 | 5 | 0.7 TPa$^{-1}$ | 0.39 TPa$^{-1}$ |
| $(\partial\kappa_s/\partial p)_T$ | BR69 | 253–268 | 0.1 | 4 | 500 TPa$^{-2}$ | 553 TPa$^{-2}$ |

[a]B12: Bridgman (1912a), B35: Bridgman (1912a, 1935), B55: Butkovich (1955), B57: Butkovich (1957), BR69: Brockamp and Rüter (1969), BT67: Brill and Tippe (1967), CWM89: Cox *et al.* (1989), D05: Dieterici (1905), D67: Dantl (1967), DG68: Dantl and Gregora (1968), DO65: Douslin and Osborn (1965), FLM60: Flubacher *et al.* (1960), G13: Griffiths (1913), GC47: Ginnings and Corruccini (1947), GKC80: Gammon *et al.* (1980, 1983), GKCW88: Gagnon *et al.* (1988), GS36: Giauque and Stout (1936), HMSS74: Haida *et al.* (1974), HS87: Henderson and Speedy (1987), JE29: Jakob and Erk (1929), JPH70: Jancso *et al.* (1970), LP60: LaPlaca and Post (1960), M34: Megaw (1934), O39: Osborne (1939), P66: Proctor (1966), REIDK94: Röttger *et al.* (1994), T55: Truby (1955).
[b]Root mean square deviation (rms) prescribed for the least-square expression of the particular data set, used for the weight of the corresponding target function. 1 TPa equals 10$^{12}$ Pa.
[c]The returned rms of the fit.

only about 1% uncertainty, measured mechanically at various ice structures above $-30\,°C$, is the only one which we used for the regression, and is in very good agreement (1%) with the current formulation.

### 3.3. Isothermal and Isentropic Compressibility

Isothermal compressibility of ice, $\kappa_T$, is obtained from specific volume and its partial pressure derivative, Eq. (12), as given in Table 3. As shown in Table 6, experimental data for $\kappa_T$ at $0\,°C$ and normal pressure vary between, e.g., 360 TPa$^{-1}$ [Bridgman (1912a)] and 120 TPa$^{-1}$ [Richards and Speyers (1914)], and this significant uncertainty remains in more recent reviews of ice properties [Dorsey (1968), Yen *et al.* (1991)]. The former Gibbs potential of Feistel and

Hagen (1995) adopted the value 232 TPa$^{-1}$ from Yen (1981), that of Tillner-Roth (1998), however, used the value 112 TPa$^{-1}$.

More reliable values are available for the isentropic compressibility, Eq. (13),

$$\kappa_s = -\frac{1}{\nu}\left(\frac{\partial\nu}{\partial p}\right)_s = \kappa_T - \frac{\alpha^2 T\nu}{c_p}, \qquad (14)$$

which can be computed from the elastic moduli of the ice lattice [see Feistel and Wagner (2005) for details]. The elastic moduli are determined acoustically or optically with high accuracy. Data at normal pressure computed from elastic constants of Dantl (1967) with uncertainties of 3%, Proctor (1966) with 1%, Brockamp and Rüter (1969) with 8%, and of Gammon *et al.* (1980) and Gagnon *et al.* (1988) with un-

a) Specific Volume at 101325 Pa



b) Deviation of Specific Volume at 101325 Pa
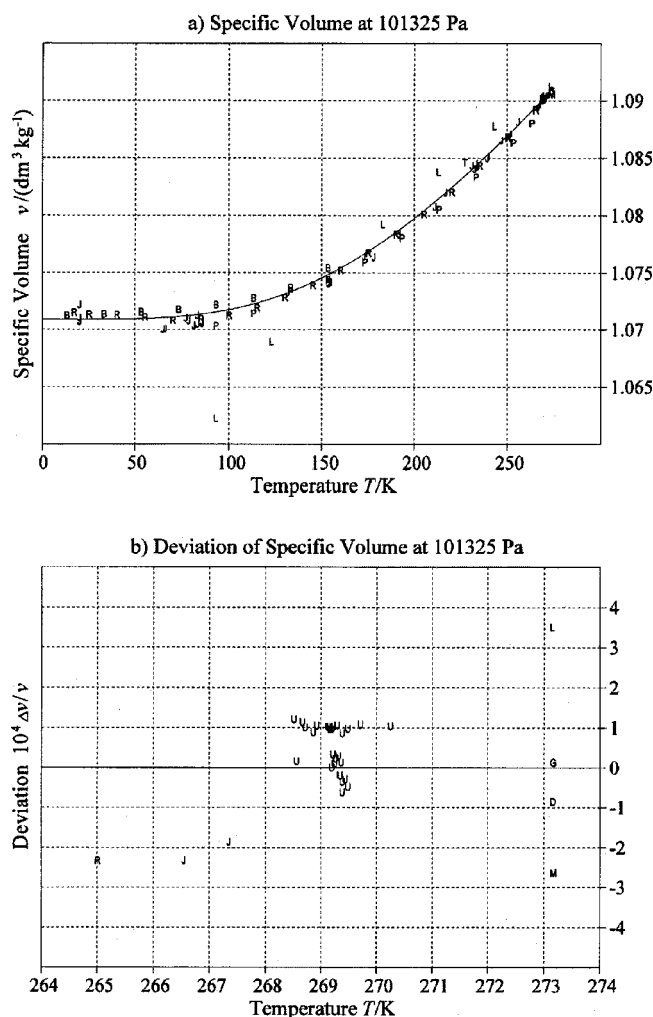
FIG. 2. Specific volume $\nu$ from Eq. (4) at normal pressure $p_0$, panel (a), and deviations $\Delta\nu/\nu=(\nu_{data}-\nu_{calc})/\nu_{calc}$ at high temperatures magnified in panel (b). Data points are B: Brill and Tippe (1967), D: Dantl and Gregora (1968), G: Ginnings and Corruccini (1947), J: Jakob and Erk (1929), L: Lonsdale (1958), M: Megaw (1934), P: LaPlaca and Post (1960), R: Röttger et al. (1994), T: Truby (1955), and U: Butkovich (1955). Most accurate data are U (estimated uncertainty 0.01%), G (0.005%), and D (0.004%).



a) Cubic Expansion Coefficient at 101325 Pa



b) Cubic Expansion Coefficient at 101325 Pa

FIG. 3. Cubic expansion coefficient $\alpha$ from Eq. (10) at normal pressure $p_0$, shown as a curve. Data points are B: Brill and Tippe (1967), D: Dantl (1962), J: Jakob and Erk (1929), P: LaPlaca and Post (1960), L: Lonsdale (1958), and R: Röttger et al. (1994). Error bars at $T>243$ K are data with uncertainties reported by Butkovitch (1957), which were used for the regression. The high-temperature part of panel (a) is magnified in panel (b).

certainties below 1% are reproduced by the current formulation within their bounds over the temperature interval 60–273 K, as are high-pressure data of Gagnon et al. (1988) at $-35\,°C$ between 0.1 and 200 MPa (Fig. 4).

## 3.4. Specific Isobaric Heat Capacity

Compared to many other solids, the heat capacity of ice Ih behaves anomalously. It follows Debye's cubic law in the zero temperature limit, but at higher temperatures it violates the empirical Grüneisen law which states that the ratio of isobaric heat capacity and isobaric thermal expansion is independent of temperature. Near the melting temperature, most crystalline solids possess a constant heat capacity, but this rule does not apply to ice. Isobaric heat capacities were

TABLE 6. Selected values reported for the isothermal compressibility $\kappa_T$ at the normal pressure melting point

| Source | $\kappa_T$ (TPa$^{-1}$) |
|---|---|
| Bridgman (1912a) | 360 |
| Richards and Speyers (1914) | 120 |
| Franks (1972) | 123 |
| Hobbs (1974) | 104 |
| Wexler (1977) | 134 |
| Yen (1981), Yen et al. (1991) | 232 |
| Henderson and Speedy (1987) | 98[a] |
| Wagner et al. (1994) | 190[a] |
| Tillner-Roth (1998) | 112 |
| Marion and Jakubowski (2004) | 140 |
| This paper | 118 |

[a]Value estimated from the curvature of the melting curve.
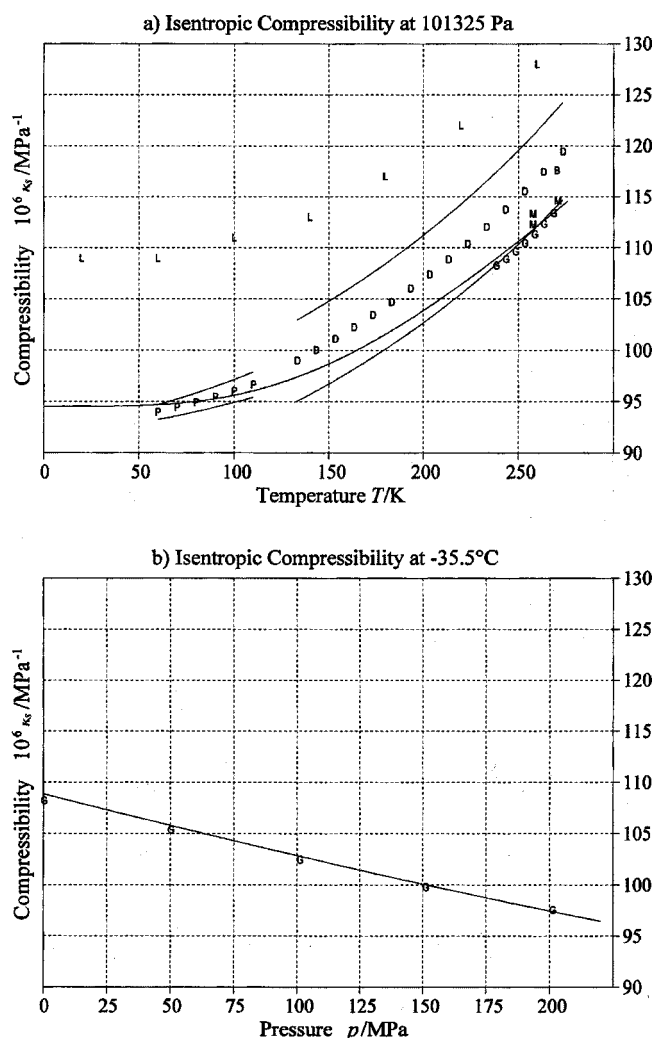
FIG. 4. Isentropic compressibilities $\kappa_s$ from Eq. (13) at normal pressure $p_0$, panel (a), and at $-35.5\,°C$, panel (b), shown as curves. D: data computed from the correlation functions for elastic moduli of Dantl (1967, 1968, 1969) with about 3% uncertainty shown as lines above and below, P: correspondingly computed data of Proctor (1966) with about 1% uncertainty, L: data of Leadbetter (1965), not used for regression, B: Brockamp and Rüter (1969), M: Gammon et al. (1980, 1983), and G: Gagnon et al. (1988).



FIG. 5. Specific isobaric heat capacity $c_p$ from Eq. (6) at normal pressure $p_0$, panel (a), shown as a curve, and relative deviation of measurements from Eq. (6), $\Delta c_p/c_p = (c_{p,\text{data}} - c_{p,\text{calc}})/c_{p,\text{calc}}$, panel (b). Data points are: G: Giauque and Stout (1936), F: Flubacher et al. (1960), S: Sugisaki et al. (1968), and H: Haida et al. (1974). The estimated experimental uncertainty of 2% is marked by solid lines.

measured at normal pressure by several authors [Giauque and Stout (1936), Flubacher et al. (1960), Sugisaki et al. (1968), Haida et al. (1974)]; all their results agree very well within their typical experimental uncertainties of about 2% (Fig. 5).

The second temperature derivative of the Gibbs potential provides the formula for the specific isobaric heat capacity, $c_p$, Eq. (6), as given in Table 3. At very low temperatures, $c_p(T)$ converges toward Debye's cubic law as

$$\lim_{T\to 0} \frac{c_p}{T^3} = 0.0091 \text{ J kg}^{-1}\text{K}^{-4}, \tag{15}$$

which is in good agreement (2%) with the corresponding limiting law coefficient $\lim_{T\to 0}(c_p/T^3) = 0.0093$ J kg$^{-1}$ K$^{-4}$ derived by Flubacher et al. (1960) from their experiment. The

equation for $c_p$ properly describes the experimental data within their uncertainty range over the entire temperature interval (Fig. 5). With this new formulation, heat capacities can be computed for arbitrary pressures, which are not available from experiments.

### 3.5. Specific Entropy

Classical thermodynamics defines entropy by heat exchange processes. This way, only entropy differences can be measured for a given substance, thus leaving absolute entropy undefined and requiring an additional reference value like the Third Law. For this reason, the IAPWS-95 formulation specifies entropy to vanish for liquid water at the triple point. Statistical thermodynamics, however, defines entropy theoretically and permits its absolute determination. For water vapor this was done by Gordon (1934) from spectroscopic data at 298.1 K and normal pressure, resulting in the

specific entropy of vapor $s^V = 45.101$ cal deg$^{-1}$ mol$^{-1}$ $= 10\,476$ J kg$^{-1}$ K$^{-1}$. The latest such value, reported by Cox *et al.* (1989), is $s^L = 69.95(3)$ J mol$^{-1}$ K$^{-1} = 3883(2)$ J kg$^{-1}$ K$^{-1}$ for the absolute entropy of liquid water at 298.15 K and 0.1 MPa, which coincides very well with $s^L = 3883.7$ J kg$^{-1}$ K$^{-1}$, as computed using the formulation of this paper, Eq. (5).

For the ice Ih crystal a theoretical residual entropy $s(0,p) = 189.13(5)$ J kg$^{-1}$ K$^{-1}$ was calculated by Pauling (1935) and Nagle (1966) from the remaining randomness of hydrogen bonds at 0 K. This value is highly consistent with Gordon's (1934) vapor entropy, as Haida *et al.* (1974) confirmed experimentally with $s(0,p) = 189.3(10.6)$ J kg$^{-1}$ K$^{-1}$ [Petrenko and Whitworth (1999)]. The theoretical residual ice entropy leads to a nonzero physical entropy of liquid water at the triple point as $s^L(T_t,p_t) = 3516(2)$ J kg$^{-1}$ K$^{-1}$, while the IAPWS-95 entropy definition for liquid water requires the residual entropy of ice to be $s(0,p) = -3327(2)$ J kg$^{-1}$ K$^{-1}$. Both versions are equally correct, but the latter value has to be used instead of the absolute one if phase equilibria between ice and fluid water are studied in conjunction with the IAPWS-95 formulation. Evidently, however, both versions differ in their uncertainties due to the different reference points.

Specific entropy $s$ is computed as temperature derivative, Eq. (5), of specific Gibbs energy, Eq. (1), as given in Table 3. Note that in this formulation entropy at 0 K is a pressure-independent constant, in accordance with theory.

At the normal melting temperature $T_{\mathrm{melt},p_0} = 273.152\,519$ K (see Sec. 3.7.), the entropy of ice $s$ can be computed from the entropy of water $s^L$, given by the IAPWS-95 formulation, and the experimental melting enthalpies $\Delta h_{\mathrm{melt}} = T_{\mathrm{melt}} \cdot (s^L - s)$ of Giauque and Stout (1936), $\Delta h_{\mathrm{melt}} = 333.49(20)$ kJ kg$^{-1}$ and $\Delta h_{\mathrm{melt}} = 333.42(20)$ kJ kg$^{-1}$, of Osborne (1939), $\Delta h_{\mathrm{melt}} = 333.54(20)$ kJ kg$^{-1}$, or of Haida *et al.* (1974), $\Delta h_{\mathrm{melt}} = 333.41$ kJ kg$^{-1}$. The melting enthalpy at $T_{\mathrm{melt},p_0}$ resulting from Eq. (7) is $\Delta h_{\mathrm{melt}} = 333.43$ kJ kg$^{-1}$ and agrees well with those data.

### 3.6. Sublimation Curve

From the equality of the chemical potentials of the solid and the gas phase,

$$g(T,p_{\mathrm{subl}}) = g^V(T,p_{\mathrm{subl}}), \qquad (16)$$

the sublimation pressure $p_{\mathrm{subl}}(T)$ can be obtained numerically, e.g., by Newton iteration, from Eq. (1) for ice and the IAPWS-95 formulation for vapor. Sublimation pressure measurements, available between 130 and 273.16 K, corresponding to 9 orders of magnitude in pressure from 200 nPa to 611 Pa, are described by the current formulation well within their experimental uncertainties (Fig. 6).

The Clausius–Clapeyron differential equation,

$$\frac{\mathrm{d}p_{\mathrm{subl}}}{\mathrm{d}T} = \frac{s - s^V}{1/\rho - 1/\rho^V}, \qquad (17)$$
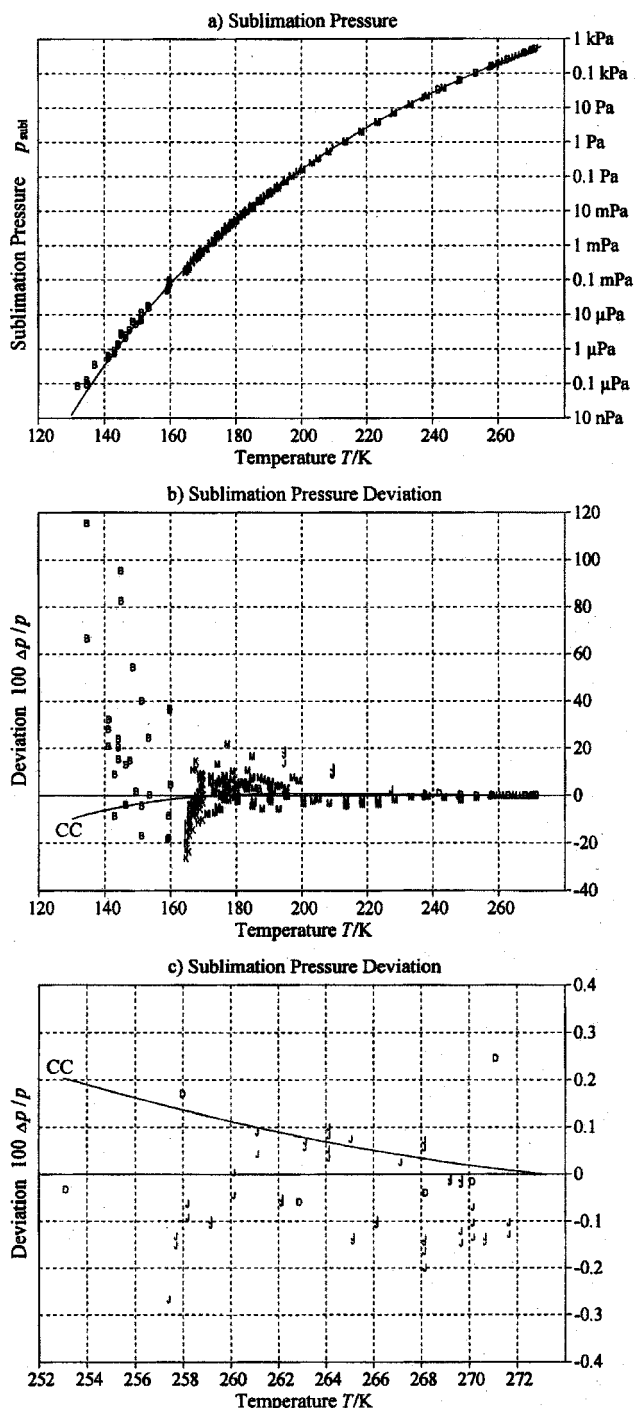


FIG. 6. Sublimation curve from the solution of Eq. (16), panel (a), and relative sublimation pressure deviations $\Delta p/p = (p_{\mathrm{data}} - p_{\mathrm{calc}})/p_{\mathrm{calc}}$, panel (b), magnified in the high-temperature range in panel (c). Data points are B: Bryson *et al.* (1974), D: Douslin and Osborn (1965), J: Jancso *et al.* (1970), K: Mauersberger and Krankowsky (2003), and M: Marti and Mauersberger (1993). For the fit only data with uncertainties of about 0.1%–0.2% were used for $T > 253$ K ($p > 100$ Pa), as shown in panel (c). Curve CC: Clausius–Clapeyron simplified sublimation law, Eq. (18).

which can be derived from Eq. (16), can be integrated in lowest order approximation, starting from the triple point $(T_t,p_t)$, under the assumptions of constant sublimation enthalpy, $\Delta h_{\mathrm{subl}} = T \cdot (s^V - s) \approx \Delta h_t = 2834.4$ kJ kg$^{-1}$, the triple

point value of this formulation, and negligible ice specific volume compared to that of the ideal gas (see Table 20 in the Appendix). The result is usually called the Clausius–Clapeyron sublimation law,

$$p_{subl}^{CC}(T) = p_t \cdot \exp\left\{ \frac{\Delta h_t}{R}\left( \frac{1}{T_t} - \frac{1}{T} \right) \right\}. \tag{18}$$

$R = 461.523\,64$ J kg$^{-1}$ K$^{-1}$ is the specific gas constant. The deviation between this very simple law, Eq. (18), and the correct sublimation pressure of this formulation, Eq. (16), is often smaller than the scatter of experimental sublimation pressure data (Fig. 6). Other, more complex sublimation formulas are in even much better agreement with the current one, like those of Jancso *et al.* (1970) for $T > 130$ K, of Wagner *et al.* (1994) for $T > 150$ K, or of Murphy and Koop (2005) for $T > 130$ K, which remain below 0.01% deviation in sublimation pressure in those temperature regions. Thus, present experimental sublimation pressure data hardly provide a suitable means for assessing the accuracy of those formulas. Sublimation enthalpy $\Delta h_{subl}$, as derived from IAPWS-95 and the current thermodynamic potential, is almost constant over a wide range of pressures and temperatures; it increases to a maximum of $\Delta h_{subl} = 2838.8$ kJ kg$^{-1}$ at 240 K and decreases again to $\Delta h_{subl} = 2810.4$ kJ kg$^{-1}$ at 150 K (Table 20), thus justifying the success of the simple equation, Eq. (18).

### 3.7. Melting Curve

The melting pressure equation of Wagner *et al.* (1994) describes the entire phase boundary between liquid water and ice Ih with an uncertainty of 3% in melting pressure. On the other hand, the freezing temperature of water and seawater derived by Feistel (2003) is more accurate at low pressures but invalid at very high pressures. The formulation given in this paper takes the benefits of both formulas, i.e., it provides the most accurate melting temperature at normal pressure and reproduces the measurements of Henderson and Speedy (1987) with 50 mK mean deviation up to 150 MPa (Fig. 7).

Melting temperature $T_{melt}$ of ice at given pressure $p$ is given by equal chemical potentials of the solid and the liquid phase,

$$g(T_{melt}, p) = g^L(T_{melt}, p), \tag{19}$$

from Eq. (1) for ice and the IAPWS-95 formulation for water. From Eq. (19), the melting temperature can be obtained numerically.

Ginnings and Corruccini (1947) measured the volume change of a water–ice mixture when heating it electrically. They determined their Bunsen calorimeter calibration factor $K_{GC47}$ to be

$$K_{GC47} = \frac{\Delta h_{melt}}{(1/\rho - 1/\rho^L)\rho_{Hg}} = 270\,415(60) \text{ J kg}^{-1} \tag{20}$$

and used it for accurate ice density determination by means of melting enthalpy $\Delta h_{melt}$, liquid water density $\rho^L$, and mercury density $\rho_{Hg}$. This way, the uncertainty of ice den-
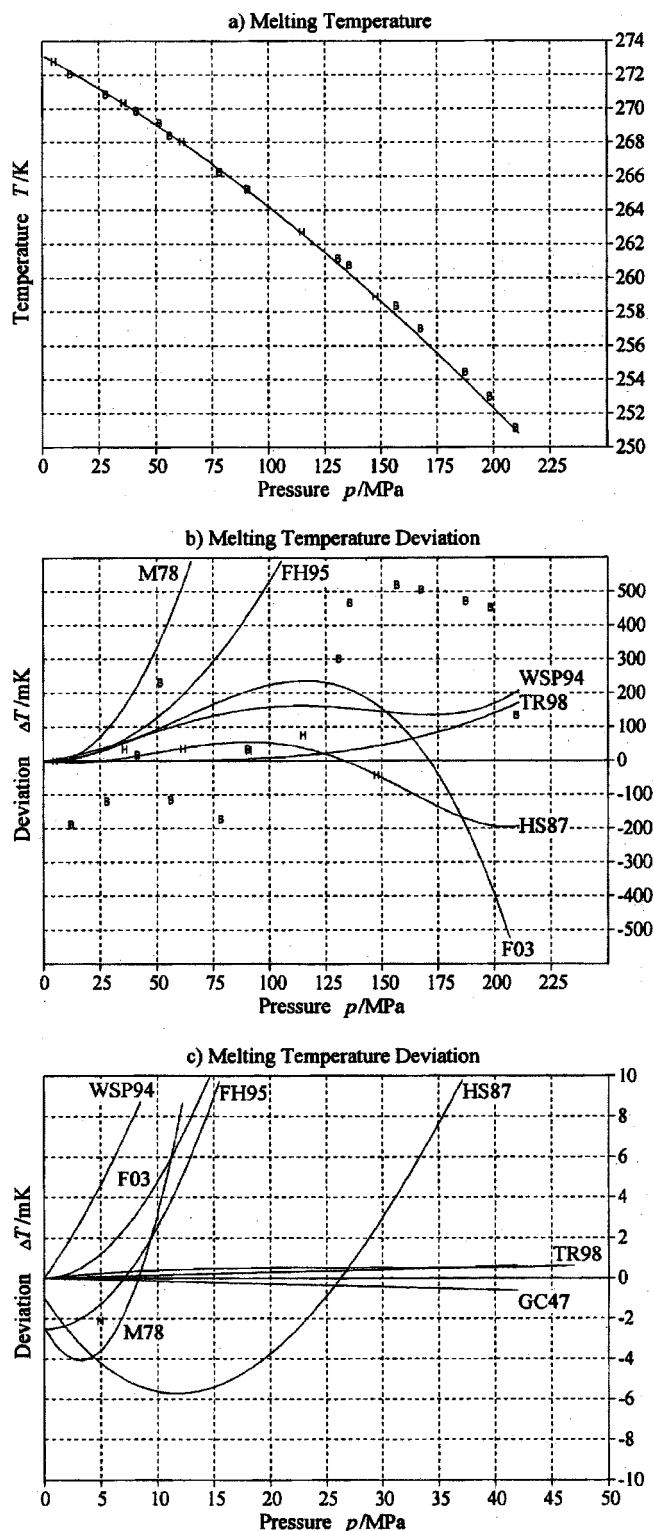


FIG. 7. Melting temperature as a function of pressure, computed from Eq. (19), shown as a curve in panel (a), and deviations $\Delta T = T_{data} - T_{calc}$ in comparison to Eq. (19) of this paper, panel (b). The low-pressure range is magnified in panel (c). Data points are: B: Bridgman (1912a), and H: Henderson and Speedy (1987). Melting curves are labeled by M78: Millero (1978), FH95: Feistel and Hagen (1995), WSP94: Wagner *et al.* (1994), TR98: Tillner-Roth (1998), HS87: Henderson and Speedy (1987), and F03: Feistel (2003). The cone labeled GC47 indicates the 0.02% uncertainty of the Clausius–Clapeyron slope at normal pressure after Ginnings and Corruccini (1947). The intercept of M78 and FH95 at normal pressure is due to the freezing temperature of air-saturated water.

sity is mainly given by the uncertainty of $\Delta h_{\text{melt}}$, namely 0.06%, while the smaller uncertainty of the calibration factor itself is only 0.02%. In Eq. (20), the original value of $K_{\text{GC47}} = 270\,370$ int.j.kg$^{-1}$ is converted from international to absolute Joules by 1.000 165 [NBS (1948), Rossini *et al.* (1952)].

The calibration factor is proportional to the Clausius–Clapeyron slope of the melting curve at normal pressure,

$$\frac{dT_{\text{melt}}}{dp} = \frac{1/\rho - 1/\rho^{\text{L}}}{s - s^{\text{L}}}$$

$$= -\frac{T_{\text{melt},p_0}}{\rho_{\text{Hg}} K_{\text{GC47}}}$$

$$= -74.301(15) \quad \text{mK MPa}^{-1}. \tag{21}$$

This value is computed with the normal pressure melting temperature $T_{\text{melt},p_0} = 273.152\,519$ K and the density of mercury, $\rho_{\text{Hg}} = 13\,595.08(2)$ kg m$^{-3}$ [PTB (1995)]. The Gibbs function of this paper provides for this melting point lowering the coefficient $\chi = -dT_{\text{melt}}/dp = 74.293$ mK MPa$^{-1}$, which fits well into the 0.02% uncertainty interval of Eq. (21). Other standard formulas like that of Bridgman (1935), $\chi = 73.21$ mK MPa$^{-1}$, of Millero (1978), $\chi = 75.3$ mK MPa$^{-1}$, or of Wagner *et al.* (1994), $\chi = 72.62$ mK MPa$^{-1}$, are significantly beyond this uncertainty limit (Fig. 7).

At normal pressure, Eq. (19) provides the melting temperature $T_{\text{melt}}(p_0) = T_{\text{melt},p_0} = 273.152\,519$ K. Making use of the fact that triple point temperature and normal pressure are exact by definition, and taking into account the small uncertainties of the triple point pressure (Table 1) and of the Clausius–Clapeyron coefficient, Eq. (21), the possible uncertainty of this normal melting temperature is estimated as only 2 $\mu$K [Feistel and Wagner (2005)]. This theoretical, very small uncertainty may practically be disguised by larger ones caused by varied isotopic composition, impurities like dissolved gases, or by natural air pressure fluctuations. In contrast, it may serve as a rather sensitive measure for the purity of ice and water in mutual equilibrium.

# 4. Uncertainties

## 4.1. Summary

Combined standard uncertainties $u_c$ reported in the following, estimated directly or indirectly from experimental data, were obtained during the numerical construction of the thermodynamic potential and exploiting its inherent consistency. Here, estimated combined standard uncertainties $u_c$ are reported [ISO (1993a)], from which expanded uncertainties $U = k u_c$ can be obtained by multiplying with the coverage factor $k = 2$, corresponding to a 95% level of confidence. The short notion "uncertainty" used in the following refers to combined standard uncertainties or to relative combined standard uncertainties.

The fundamental information about the uncertainty of a particular quantity in a certain region of the $T$-$p$ space is adopted from the uncertainties reported or estimated for the most accurate related experimental data. If such uncertainties were unavailable or inappropriate, our estimates were based on the quantitative agreement and consistency of the data considered, with respect to the present formulation. For cases without any corresponding measurements, attempts were made to derive the required uncertainties from other, measured parameters using thermodynamic rules. For these quantities in particular, more detailed derivations are described below.

A summary of estimated combined standard uncertainties of selected quantities in certain regions of the $T$-$p$ space is given in Table 7. The uncertainty of density in different regions of the $T$-$p$ space is shown in Fig. 8.

## 4.2. Uncertainty of Specific Entropy

Uncertainties of specific entropy are different, depending on the reference state chosen, either "IAPWS-95" or "absolute." For both cases, we estimate uncertainties at specifically selected $T$-$p$ conditions. Uncertainty estimates for differences $\Delta s$ of specific entropy, corresponding to thermodynamic transition processes between the initial and the final states as given in Tables 8 and 9, do not depend on the choice of the reference state and are valid for both cases: IAPWS-95 or absolute. In particular, we derive a value for the uncertainty of the specific entropy difference $\Delta s$ between the zero point and the melting point,

$$u_c(\Delta s) = u_c[s(T_{\text{melt},p_0}, p_0) - s(0, p_0)]. \tag{22}$$

In Table 8, it is assumed that the specific zero-point entropy with its uncertainty [Pauling (1935), Nagle (1966)] is given. All other specific entropy values are computed relative to it using the present and the IAPWS-95 formulation. The specific entropy uncertainty at the CODATA point is adopted from Cox *et al.* (1989). The uncertainty of its specific entropy difference to the freezing point is estimated as

$$u_c[s^{\text{L}}(298.15 \text{ K}, p_0) - s^{\text{L}}(T_{\text{melt},p_0}, p_0)]$$

$$= \int_{T_{\text{melt},p_0}}^{298.15 \text{ K}} \frac{u_c(c_p^{\text{L}})}{T} dT$$

$$\approx 4 \text{ J kg}^{-1} \text{ K}^{-1} \cdot \ln\frac{298.15 \text{ K}}{T_{\text{melt},p_0}}$$

$$\approx 0.4 \text{ J kg}^{-1} \text{ K}^{-1} \tag{23}$$

using the heat capacity uncertainty of 0.1% (IAPWS-95), i.e., $u_c(c_p^{\text{L}}) = 4$ J kg$^{-1}$ K$^{-1}$. For the specific freezing point entropy, the uncertainty of 1.8 J kg$^{-1}$ K$^{-1}$ is computed as the root mean square of 0.4 J kg$^{-1}$ K$^{-1}$ and 1.7 J kg$^{-1}$ K$^{-1}$. With the additional specific melting entropy uncertainty of only 0.07 J kg$^{-1}$ K$^{-1}$ due to Giauque and Stout (1936), the uncertainty of the specific melting point entropy remains 1.8 J kg$^{-1}$ K$^{-1}$. Together with the specific zero point entropy uncertainty of only 0.05 J kg$^{-1}$ K$^{-1}$, we finally get the uncertainty of the specific entropy difference between the zero point and the melting point to be

TABLE 7. Summary of estimated combined standard uncertainties of selected quantities in certain regions of the $T$-$p$ space, derived from corresponding experiments

| Quantity | $T$ interval | $p$ interval | Uncertainty |
|---|---|---|---|
| $u_c(g)$ | $T \leqslant 273$ K | $p \leqslant 0.1$ MPa | $2$ J kg$^{-1}$ K$^{-1} \times |T - T_t|$ |
| $u_c(g)$ | $238$ K $\leqslant T \leqslant 273$ K | $p \leqslant 200$ MPa | $2$ J kg$^{-1}$ K$^{-1} \times |T - T_t| + 2 \times 10^{-6}$ J kg$^{-1}$ Pa$^{-1}$ $\times |p - p_t|$ |
| $u_c(h)$ | $T \leqslant 273$ K | $p \leqslant 0.1$ MPa | $600$ J kg$^{-1}$ |
| $u_c(\Delta h_{melt})$ | $T = 273.15$ K | $p = 0.1$ MPa | $200$ J kg$^{-1}$ |
| $u_c(\Delta h_{subl})$ | $130$ K $\leqslant T \leqslant 273$ K | $100$ nPa $\leqslant p$ | $4$ J kg$^{-1}$ K$^{-1} \times T$ |
| $u_c(dp_{melt}/dT)$ | $T = 273.15$ K | $p = 0.1$ MPa | $3 \times 10^3$ Pa K$^{-1}$ |
| $u_c(T_{melt})$ | $273.15$ K $\leqslant T$ | $p \leqslant 0.1$ MPa | $2 \times 10^{-6}$ K[a] |
| $u_c(T_{melt})$ | $273.11$ K $\leqslant T$ | $p \leqslant 0.6$ MPa | $40 \times 10^{-6}$ K |
| $u_c(T_{melt})$ | $266$ K $\leqslant T \leqslant 273$ K | $p \leqslant 100$ MPa | $2 \times 10^{-9}$ K Pa$^{-1} \times p$ |
| $u_c(T_{melt})$ | $259$ K $\leqslant T \leqslant 266$ K | $100$ MPa $\leqslant p \leqslant 150$ MPa | $0.5$ K |
| $u_c(p_{melt})/p_{melt}$ | $266$ K $\leqslant T \leqslant 273$ K | $p \leqslant 100$ MPa | $2\%$ |
| $u_c(p_{subl})$ | $257$ K $\leqslant T \leqslant 273$ K | $100$ Pa $\leqslant p$ | $0.4$ Pa |
| $u_c(p_{subl})/p_{subl}$ | $130$ K $\leqslant T \leqslant 257$ K | $100$ nPa $\leqslant p \leqslant 100$ Pa | $0.6\%$ |
| $u_c(s)$ | $T \leqslant 273$ K | $p \leqslant 0.1$ MPa | $2$ J kg$^{-1}$ K$^{-1}$ |
| $u_c(c_p)/c_p$ | $T \leqslant 273$ K | $p \leqslant 0.1$ MPa | $2\%$ |
| $u_c(\rho)/\rho$ | $268$ K $\leqslant T \leqslant 273$ K | $p \leqslant 0.1$ MPa | $0.02\%$ |
| $u_c(\rho)/\rho$ | $T \leqslant 268$ K | $p \leqslant 0.1$ MPa | $0.1\%$ |
| $u_c(\rho)/\rho$ | $238$ K $\leqslant T \leqslant 273$ K | $p \leqslant 200$ MPa | $0.2\%$ |
| $u_c(\alpha)$ | $243$ K $\leqslant T \leqslant 273$ K | $p \leqslant 0.1$ MPa | $2 \times 10^{-6}$ K$^{-1}$ |
| $u_c(\alpha)$ | $100$ K $\leqslant T \leqslant 243$ K | $p \leqslant 0.1$ MPa | $5 \times 10^{-6}$ K$^{-1}$ |
| $u_c(\kappa_s), u_c(\kappa_T)$ | $60$ K $\leqslant T \leqslant 273$ K | $p \leqslant 0.1$ MPa | $1 \times 10^{-12}$ Pa$^{-1}$ |
| $u_c(\kappa_s), u_c(\kappa_T)$ | $238$ K $\leqslant T \leqslant 273$ K | $p \leqslant 200$ MPa | $1 \times 10^{-12}$ Pa$^{-1}$ |

[a]Value assumes an exact triple point temperature. If isotopic variations are accounted for, the additional uncertainty of the triple point temperature of $40$ $\mu$K must be included, see text.
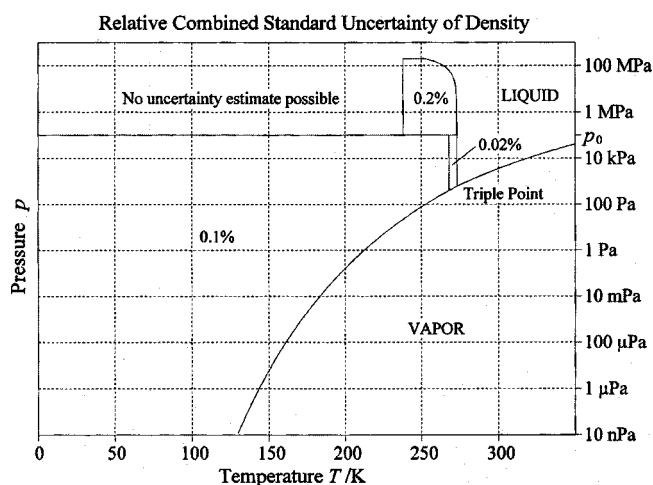


FIG. 8. Relative combined standard uncertainty of ice density, $u_c(\rho)/\rho$, Table 7, estimated for different regions of the $T$-$p$ space. No experimental high-pressure data are available at low temperatures.

$$u_c[s(T_{melt,p_0}, p_0) - s(0, p_0)] = 1.8 \ \text{J kg}^{-1} \text{K}^{-1}. \quad (24)$$

This value, which is derived from essentially the uncertainties of the specific absolute entropies at the zero point and the CODATA point, is significantly smaller than the usual value of $12$ J kg$^{-1}$ K$^{-1}$ given by Giauque and Stout (1936), obtained from the heat capacity uncertainty.

If, however, entropy is subject to the IAPWS-95 reference state, its value for the liquid phase at the triple point is zero by definition (Table 9). The uncertainty of specific entropy at the freezing point then follows from the path integral between the adjacent states,

$$u_c[s^L(T_t, p_t) - s^L(T_{melt,p_0}, p_0)]$$
$$= \int_{T_{melt,p_0}}^{T_t} \frac{u_c(c_p^L)}{T} dT + \int_{p_0}^{p_t} u_c\left[\left(\frac{\partial v^L}{\partial T}\right)_p\right] dp$$
$$\approx 4 \ \text{J kg}^{-1} \text{K}^{-1} \cdot \left| \ln \frac{T_t}{T_{melt,p_0}} \right|$$

TABLE 8. Uncertainties $u_c$ of absolute specific entropies $s$ and of their differences $\Delta s$

| | $T$ (K) | $p$ (Pa) | $\Delta s$ (J kg$^{-1}$ K$^{-1}$) | $s$ (J kg$^{-1}$ K$^{-1}$) | $u_c$ (J kg$^{-1}$ K$^{-1}$) |
|---|---|---|---|---|---|
| Zero point | 0 | 101 325 | | 189.13 | 0.05 |
| Difference | | | 2106.57 | | 1.8 |
| Melting point | 273.152 519 | 101 325 | | 2295.70 | 1.8 |
| Melting | | | 1220.67 | | 0.07 |
| Freezing point | 273.152 519 | 101 325 | | 3516.37 | 1.8 |
| Difference | | | 367.31 | | 0.4 |
| CODATA point | 298.15 | 100 000 | | 3883.67 | 1.7 |

TABLE 9. Uncertainties $u_c$ of IAPWS-95 specific entropies $s$ and of their differences $\Delta s$

| | $T$ (K) | $p$ (Pa) | $\Delta s$ (J kg$^{-1}$ K$^{-1}$) | $s$ (J kg$^{-1}$ K$^{-1}$) | $u_c$ (J kg$^{-1}$ K$^{-1}$) |
|---|---|---|---|---|---|
| Zero point | 0 | 101 325 | | $-3327.34$ | 1.8 |
| Difference | | | 2106.57 | | 1.8 |
| Melting point | 273.152 519 | 101 325 | | $-1220.77$ | 0.07 |
| Melting | | | 1220.67 | | 0.07 |
| Freezing point | 273.152 519 | 101 325 | | $-0.11$ | 0.0002 |
| Difference | | | 0.11 | | 0.0002 |
| Triple point | 273.16 | 611.657 | | 0.0 | 0.0 |

$$+ |p_t - p_0| \cdot 6 \cdot 10^{-10} \text{ m kg}^{-1} \text{ K}^{-1}$$

$$\approx 0.0002 \text{ J kg}^{-1} \text{ K}^{-1}. \tag{25}$$

The uncertainty of specific heat capacity was taken from the IAPWS-95 formulation, that of thermal expansion was derived from the measurements of Caldwell (1978), see Feistel (2003), thus resulting in an uncertainty of 0.0002 J kg$^{-1}$ K$^{-1}$ of specific entropy at the freezing point. The uncertainty of the specific melting entropy of Giauque and Stout (1936) of 0.07 J kg$^{-1}$ K$^{-1}$ is then the dominant contribution to the uncertainty 0.07 J kg$^{-1}$ K$^{-1}$ of specific entropy at the melting point. Between this point and the zero point, the uncertainty of the specific entropy difference was determined in Table 8 to be 1.8 J kg$^{-1}$ K$^{-1}$. Therefore, the uncertainty of the specific residual entropy with respect to the IAPWS-95 reference state is 1.8 J kg$^{-1}$ K$^{-1}$.

### 4.3. Uncertainty of Specific Gibbs Energy

The specific Gibbs energy of arbitrary $T$-$p$ states can be computed by the path integral starting from the triple point,

$$g(T,p) = g(T_t, p_t) - \int_{T_t}^{T} s(T', p_t) dT' + \int_{p_t}^{p} \nu(T, p') dp'. \tag{26}$$

The corresponding uncertainties can be computed, using values given in Table 7, for the specific Gibbs energy

$$u_c[g(T_t, p_t)] = u_c[u(T_t, p_t) - T_t s(T_t, p_t) + p_t \nu(T_t, p_t)]$$

$$= p_t u_c[\nu(T_t, p_t)] + \nu(T_t, p_t) u_c(p_t), \tag{27}$$

$$u_c[g(T_t, p_t)] = 13 \cdot 10^{-5} \text{ J kg}^{-1}, \tag{28}$$

for the specific entropy,

$$u_c[s(T, p_t)] = 2 \text{ J kg}^{-1} \text{ K}^{-1}, \tag{29}$$

and for the specific volume,

$$u_c[\nu(T,p)] = 0.2 \text{ J kg}^{-1} \text{ MPa}^{-1} \text{ for } 268 \text{ K} \leqslant T \leqslant 273 \text{ K},$$

$$p \leqslant 0.1 \text{ MPa}, \tag{30}$$

$$u_c[\nu(T,p)] = 1 \text{ J kg}^{-1} \text{ MPa}^{-1} \text{ for } T \leqslant 268 \text{ K},$$

$$p \leqslant 0.1 \text{ MPa}, \tag{31}$$

and

$$u_c[\nu(T,p)] = 2 \text{ J kg}^{-1} \text{ MPa}^{-1} \text{ for } 238 \text{ K} \leqslant T \leqslant 273 \text{ K},$$

$$p \leqslant 200 \text{ MPa}. \tag{32}$$

So we get for the three different regions the expressions $268 \text{ K} \leqslant T \leqslant 273 \text{ K}$, $p \leqslant 0.1$ MPa:

$$u_c(g) = 13 \cdot 10^{-5} \text{ J kg}^{-1} + 2 \text{ J kg}^{-1} \text{ K}^{-1} |T - T_t|$$

$$+ 0.2 \text{ J kg}^{-1} \text{ MPa}^{-1} |p - p_t|, \tag{33}$$

$T \leqslant 268 \text{ K}$, $p \leqslant 0.1$ MPa:

$$u_c(g) = 13 \cdot 10^{-5} \text{ J kg}^{-1} + 2 \text{ J kg}^{-1} \text{ K}^{-1} |T - T_t|$$

$$+ 1 \text{ J kg}^{-1} \text{ MPa}^{-1} |p - p_t|, \tag{34}$$

$238 \text{ K} \leqslant T \leqslant 273 \text{ K}$, $p \leqslant 200$ MPa:

$$u_c(g) = 13 \cdot 10^{-5} \text{ J kg}^{-1} + 2 \text{ J kg}^{-1} \text{ K}^{-1} |T - T_t|$$

$$+ 2 \text{ J kg}^{-1} \text{ MPa}^{-1} |p - p_t|. \tag{35}$$

Usually, these terms can be safely simplified to those given in Table 7.

### 4.4. Uncertainty of Specific Enthalpy

Expressing specific enthalpy by $h = g + Ts$, we can estimate its uncertainty as

$$u_c(h) = u_c(g) + T u_c(s) \approx 2 \text{ J kg}^{-1} \text{ K}^{-1} |T - T_t|$$

$$+ 2 \text{ J kg}^{-1} \text{ K}^{-1} T = 2 \text{ J kg}^{-1} \text{ K}^{-1} T_t \approx 600 \text{ J kg}^{-1} \tag{36}$$

in the low-pressure region $T \leqslant 273$ K, $p \leqslant 0.1$ MPa.

### 4.5. Uncertainty of Sublimation Enthalpy

The uncertainty of specific entropy of ice below 0.1 MPa, and therefore along the sublimation curve as well, is 1.8 J kg$^{-1}$ K$^{-1}$. Supposing the IAPWS-95 specific heat capacity of water vapor at low pressures to be known with an uncertainty of $u_c(c_p^V)/c_p^V \approx 0.03\%$ and the evaporation entropy of about 9 kJ kg$^{-1}$ K$^{-1}$ with an uncertainty of 0.02%, we get for the specific entropy of vapor an uncertainty estimate of

$$u_c[s^V(T,p)] = u_c\left[s^V(T_t,p) + \int_{T_t}^{T}(c_p^V/T)dT\right]$$

$$\approx u_c[s^V(T_t,p_t)] + u_c(c_p^V)\ln(T_t/T)$$

$$\approx 2 \ \text{J kg}^{-1}\text{K}^{-1} + (T_t - T)\cdot 0.004 \ \text{J kg}^{-1}\text{K}^{-2}. \tag{37}$$

Summing up the ice and vapor parts, the uncertainty estimate of sublimation enthalpy is

$$u_c(\Delta h_{subl}) = T u_c(\Delta s_{subl})$$

$$\approx T\left(1 - \frac{T}{1250 \ \text{K}}\right)\cdot 5 \ \text{J kg}^{-1}\text{K}^{-1}$$

$$\approx T\cdot 4 \ \text{J kg}^{-1}\text{K}^{-1}, \tag{38}$$

varying between about 0.4 kJ kg$^{-1}$ (or 0.015%) at 130 K and 1 kJ kg$^{-1}$ (or 0.03%) at 273 K.

### 4.6. Uncertainty of Sublimation Pressure

For an estimate of the uncertainty of the sublimation pressure above 100 Pa, we adopt the value 0.4 Pa as provided by Jancso *et al.* (1970) for his experiment. Below 100 Pa, we use the Clausius–Clapeyron differential equation, Eq. (17),

$$\frac{dp_{subl}}{dT} = \frac{s^V - s}{\nu^V - \nu} \tag{39}$$

in an approximate form with $\nu^V - \nu \approx \nu^V \approx RT/p$,

$$\frac{u_c[p_{subl}]}{p_{subl}} \approx \left|\int_{T_t}^{T} u_c(\Delta s_{subl})\frac{dT'}{RT'}\right|$$

$$\approx \frac{u_c(\Delta s_{subl})}{R}\ln\frac{T_t}{T}$$

$$\approx 0.9\%\cdot\ln\frac{T_t}{T}. \tag{40}$$

Therefore, down to 130 K, we can estimate the relative uncertainty by $u_c[p_{subl}]/p_{subl} = 0.6\%$. This value is smaller than the usual experimental scatter, which is between 1% and 10% of the sublimation pressure at low temperatures [Mauersberger and Krankowski (2003), Marti and Mauersberger (1993)].

### 4.7. Uncertainties of Melting Temperature and Pressure

Melting temperatures cannot be more accurate than the triple point temperature, which is theoretically exact by definition, but in practice uncertain within about 0.04 mK due to isotopic variations [Nicholas *et al.* (1996), White *et al.* (2003)]. In the linear range of the melting curve, the experimental uncertainty of the Clausius–Clapeyron slope of the melting curve at normal pressure, Eq. (21), gives rise to uncertainties of the melting temperatures which are even smaller than 0.04 mK (Table 7). At higher pressures, about

$p > 0.6$ MPa, when the effect of the curvature of the melting curve becomes comparable with that uncertainty, a more general estimate is required.

The melting curve is determined by the vanishing chemical potential difference

$$\Delta g = g^L(T,p) - g(T,p)$$

$$= \int_{p_t}^{p}\nu^L(T_t,p')dp' - \int_{T_t}^{T}s^L(T',p)dT'$$

$$+ \int_{T_t}^{T}s(T',p_t)dT' - \int_{p_t}^{p}\nu(T,p')dp'. \tag{41}$$

The two integration paths are chosen to be inside the liquid and inside the vapor region of the $T$-$p$ space. Since no uncertainty estimate is given by the IAPWS-95 formulation for the specific entropy of the liquid, we transform by partial integration the corresponding integral into

$$\int_{T_t}^{T}s^L(T',p)dT' = \int_{T_t}^{T}\left(\frac{T}{T'} - 1\right)c_p^L(T',p)dT'. \tag{42}$$

For $p \le 100$ MPa, we can estimate the uncertainty $u_c(\Delta g)$ using the values $u_c(\nu^L)/\nu^L = 0.003\%$ (from IAPWS-95), $u_c(c_p^L)/c_p^L = 0.3\%$ (from IAPWS-95), $u_c(\nu)/\nu = 0.2\%$ (from Table 7), and, at $p \le 0.1$ MPa, $u_c(s) = 2$ J kg$^{-1}$K$^{-1}$ (from Table 7):

$$u_c(\Delta g) = \int_{p_t}^{p}u_c[\nu^L(T_t,p')]dp'$$

$$+ \int_{T_t}^{T}\left(\frac{T}{T'} - 1\right)u_c[c_p^L(T',p)]dT'$$

$$+ \int_{T_t}^{T}u_c[s(T',p_t)]dT' + \int_{p_t}^{p}u_c[\nu(T,p')]dp' \tag{43}$$

$$u_c(\Delta g) = 3\cdot 10^{-8} \ \text{m}^3\text{kg}^{-1}(p - p_t)$$

$$+ 12 \ \text{J kg}^{-1}\text{K}^{-1}\left(T\ln\frac{T}{T_t} - T + T_t\right)$$

$$+ 2 \ \text{J kg}^{-1}\text{K}^{-1}|T - T_t|$$

$$+ 2\cdot 10^{-6} \ \text{m}^3\text{kg}^{-1}(p - p_t). \tag{44}$$

Along the melting curve up to 100 MPa, the last of these four terms is clearly dominating, which results from the uncertainty of the ice density at high pressures. At given pressure, the uncertainty in melting temperature becomes

$$u_c(\Delta g) = |\Delta s_{melt}|u_c(T_{melt})$$

$$= \left|\frac{\Delta h_{melt}}{T_{melt}}\right|u_c(T_{melt})$$

$$= 2\cdot 10^{-6} \ \text{m}^3\text{kg}^{-1}(p - p_t), \tag{45}$$

$$u_c(T_{melt}) \approx 2\cdot 10^{-9} \ \text{K Pa}^{-1}\cdot p. \tag{46}$$

Particularly in the medium pressure range, this uncertainty is much smaller than $u_c(T_{melt}) = 0.5$ K given by Henderson and Speedy (1987) for their data.

At a given temperature, this corresponds to the relative uncertainty of the melting pressure,

$$u_c(\Delta g) = |\Delta \nu_{melt}| u_c(p_{melt})$$

$$= 2 \cdot 10^{-6} \text{ m}^3 \text{ kg}^{-1}(p_{melt} - p_t), \quad (47)$$

$$\frac{u_c(p_{melt})}{p_{melt}} = 2\%. \quad (48)$$

This value, derived here without explicitly considering any freezing point measurements, is in good agreement with $u_c(p_{melt})/p_{melt} = 3\%$ reported by Wagner *et al.* (1994).

## 5. Conclusion

A new, compact analytical formulation for the Gibbs thermodynamic potential of ice Ih is presented. It is valid in temperature between 0 and 273.16 K and in pressure between 0 and 210 MPa, thus covering the entire region of stable existence in the $T$-$p$ diagram. Combining various properties into a single, consistent formula allows significantly reduced uncertainties for properties (such as isothermal compressibility and thermal expansion coefficient), where the direct experimental measurements have relatively high uncertainty. Combined with the IAPWS-95 formulation of fluid water, accurate values for melting and sublimation points can be derived in a consistent manner, replacing former separate correlation functions. This method can directly be extended to other aqueous systems like seawater. Thus, a Gibbs function of sea ice and the freezing points of seawater are made available up to 100 MPa [Feistel and Wagner (2005), Feistel *et al.* (2005)].

Five hundred twenty two data points of 32 different groups of measurements are reproduced by the new formulation within their experimental uncertainty. The formulation obeys Debye's theoretical cubic law at low temperatures, and pressure-independent residual entropy as required by the Third Law. By deriving it from very accurately known elastic lattice constants of ice, the uncertainty in isothermal compressibility of previous formulas is reduced by about 100 times; its new value at normal pressure is 118(1) $\text{TPa}^{-1}$. The uncertainty in the Clausius–Clapeyron slope $\chi$ at normal pressure of previous formulas is reduced by 100 times; for the melting point lowering at normal pressure the Gibbs function of this paper provides the coefficient $\chi = 74.293$ mK $\text{MPa}^{-1}$ with 0.02% uncertainty. The absolute entropy of liquid water at the triple point is found to be 3516(2) $\text{J kg}^{-1} \text{K}^{-1}$. The corresponding figure of absolute entropy of liquid water at 298.15 K and 0.1 MPa is 3883.7 $\text{J kg}^{-1} \text{K}^{-1}$; it agrees very well with the latest CODATA key value, 3882.8(1.7) $\text{J kg}^{-1} \text{K}^{-1}$ [Cox *et al.* (1989)].

The melting temperature at normal pressure is found to be 273.152 519(2) K if the triple point temperature is supposed to be exact by definition. The deviation of experimental melting points at high pressures is about 50 mK; the uncertainty of the present formulation is estimated as 2% of the melting pressure. The density of ice at the normal pressure melting point is 916.72 $\text{kg m}^{-3}$ with an estimated uncertainty of 0.01%, in excellent agreement with the value computed by Ginnings and Corruccini (1947).

Density measurements of different authors deviate by up to 0.3% in an apparently systematic manner. The hypothetical shallow density maximum at about 70 K is not reflected in this formulation, further investigation of this point seems in order for its decisive clarification, possibly in conjunction with an improved knowledge about the supposed phase transition to ice XI. The deviations in measured heat capacity at the apparent transition point at about 100 K appear to be systematic but do not rise above the average experimental uncertainty threshold. Further work is apparently required to resolve those deviations for being included into the theoretical formulation. The heat capacity $c_p$ at high pressures barely deviates from its low-pressure values; the differences are within the 2% uncertainty of $c_p$ at normal pressure.

An extension of the sublimation curve to lower temperatures and pressures will require data of water vapor heat capacities below 130 K which are not implemented in the current IAPWS-95 formulation. The $c_p^V$ value at 130 K is about $4R$ [Wagner and Pruß (2002)] and must decrease exponentially to $1.5R$ at 0 K due to successively vanishing contributions from vibrational and rotational excitation states of the water molecules [Landau and Lifschitz (1966)]. Points of this curve, required for the computation of the chemical potential of water vapor, are known down to a $c_p^V$ value of about $3R$ at 10 K [Woolley (1980)].

Experimental data for ice Ih at high pressures and low temperatures are completely missing. Phase transition curves in this region are only very vaguely known by now. Verifying the current quantitative knowledge in those "white areas" of the $T$-$p$ diagram remains a future task.

are freely available as source code examples from the numerical supplement of a web-published article by Feistel *et al.* (2005).

# 7. Appendix: Tables and Diagrams of Thermodynamic Properties of Ice Ih

The new formulation provides properties of ice Ih which have previously been measured only partly, if at all. For an overview, in this section the most important quantities derived from the potential function are provided as tables as well as displayed graphically as functions of temperature and pressure. Given are the Gibbs energy (Table 10, Fig. 9), the density (Table 11, Fig. 10), the specific entropy (Table 12, Fig. 11), the specific isobaric heat capacity (Table 13, Fig. 12), the specific enthalpy (Table 14, Fig. 13), the cubic expansion coefficient (Table 15, Fig. 14), the pressure coefficient (Table 16, Fig. 15), and the isothermal compressibility (Table 17, Fig. 16). Sublimation equilibrium states exist for arbitrarily small pressures $p>0$. The values reported in the column "0 Pa" refer to ice properties in the mathematical limit of an infinitely small pressure $p$.

Equilibria between ice and liquid water or water vapor require equal chemical potentials of water between those phases, which are available from the IAPWS-95 Gibbs energy of pure water, $g^L(T,p)$, and of water vapor, $g^V(T,p)$
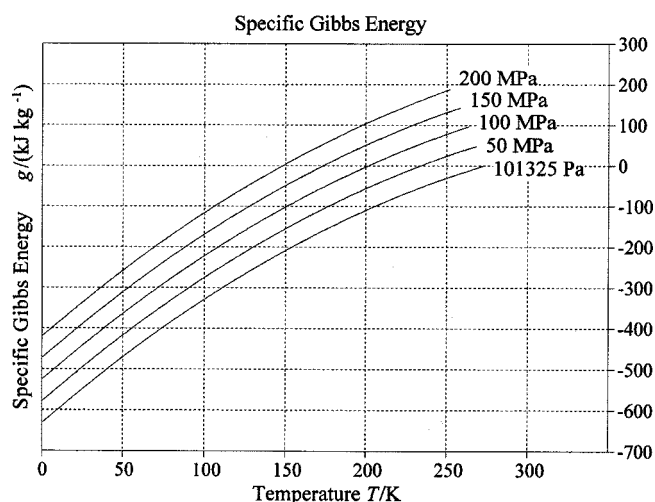


FIG. 9. Specific Gibbs energy $g(T,p)$ of ice, i.e., its chemical potential, in kJ kg$^{-1}$ as a function of temperature for several pressures as indicated at the curves. Values were computed from Eq. (1).

(Wagner and Pruß 2002). In such cases, the Gibbs function of ice must be evaluated using the IAPWS-95 version of the residual entropy coefficient $s_0$ (Table 2). Therefore, the IAPWS-95 reference state with vanishing entropy and internal energy of liquid water at the triple point, Eq. (2), was

TABLE 10. Specific Gibbs energy, $g(T,p)$, Eq. (1), in kJ kg$^{-1}$

| Temp. (K) | Pressure | | | | | |
|---|---|---|---|---|---|---|
| | 0 Pa | 101 325 Pa | 50 MPa | 100 MPa | 150 MPa | 200 MPa |
| 0 | −632.129 | −632.020 | −578.708 | −525.530 | −472.583 | −419.860 |
| 10 | −598.865 | −598.757 | −545.445 | −492.266 | −439.320 | −386.596 |
| 20 | −565.778 | −565.670 | −512.357 | −459.179 | −406.233 | −353.509 |
| 30 | −533.227 | −533.119 | −479.806 | −426.628 | −373.681 | −320.957 |
| 40 | −501.435 | −501.326 | −448.013 | −394.834 | −341.886 | −289.162 |
| 50 | −470.483 | −470.375 | −417.060 | −363.879 | −310.930 | −258.205 |
| 60 | −440.405 | −440.297 | −386.979 | −333.796 | −280.845 | −228.117 |
| 70 | −411.214 | −411.106 | −357.783 | −304.595 | −251.641 | −198.909 |
| 80 | −382.914 | −382.805 | −329.476 | −276.282 | −223.321 | −170.584 |
| 90 | −355.503 | −355.394 | −302.055 | −248.851 | −195.882 | −143.137 |
| 100 | −328.974 | −328.866 | −275.513 | −222.297 | −169.316 | −116.561 |
| 110 | −303.320 | −303.212 | −249.841 | −196.608 | −143.613 | −90.845 |
| 120 | −278.529 | −278.420 | −225.027 | −171.774 | −118.760 | −65.975 |
| 130 | −254.589 | −254.480 | −201.060 | −147.783 | −94.746 | −41.940 |
| 140 | −231.488 | −231.379 | −177.928 | −124.621 | −71.557 | −18.728 |
| 150 | −209.215 | −209.106 | −155.618 | −102.278 | −49.183 | 3.675 |
| 160 | −187.759 | −187.650 | −134.121 | −80.743 | −27.613 | 25.277 |
| 170 | −167.112 | −167.003 | −113.428 | −60.007 | −6.839 | 46.087 |
| 180 | −147.266 | −147.157 | −93.532 | −40.064 | 13.148 | 66.113 |
| 190 | −128.214 | −128.105 | −74.425 | −20.907 | 32.352 | 85.359 |
| 200 | −109.951 | −109.842 | −56.103 | −2.530 | 50.778 | 103.832 |
| 210 | −92.472 | −92.363 | −38.562 | 15.070 | 68.432 | 121.535 |
| 220 | −75.774 | −75.664 | −21.797 | 31.896 | 85.316 | 138.472 |
| 230 | −59.853 | −59.743 | −5.806 | 47.952 | 101.432 | 154.643 |
| 240 | −44.706 | −44.596 | 9.413 | 63.240 | 116.783 | 170.053 |
| 250 | −30.333 | −30.222 | 23.863 | 77.761 | 131.371 | 184.702 |
| 260 | −16.730 | −16.619 | 37.546 | 91.518 | — | — |
| 270 | −3.896 | −3.785 | — | — | — | — |
| 273 | −0.195 | −0.085 | — | — | — | — |

TABLE 11. Density, $\rho(T,p)$, Eq. (4), in kg m$^{-3}$

| Temp. (K) | Pressure | | | | | |
|---|---|---|---|---|---|---|
| | 0 Pa | 101 325 Pa | 50 MPa | 100 MPa | 150 MPa | 200 MPa |
| 0 | 933.79 | 933.80 | 938.13 | 942.32 | 946.37 | 950.29 |
| 10 | 933.79 | 933.80 | 938.13 | 942.32 | 946.37 | 950.29 |
| 20 | 933.79 | 933.79 | 938.12 | 942.32 | 946.37 | 950.29 |
| 30 | 933.78 | 933.79 | 938.12 | 942.31 | 946.36 | 950.28 |
| 40 | 933.77 | 933.78 | 938.11 | 942.30 | 946.35 | 950.27 |
| 50 | 933.74 | 933.75 | 938.08 | 942.28 | 946.33 | 950.25 |
| 60 | 933.69 | 933.69 | 938.03 | 942.23 | 946.29 | 950.22 |
| 70 | 933.60 | 933.61 | 937.95 | 942.16 | 946.22 | 950.16 |
| 80 | 933.47 | 933.48 | 937.83 | 942.05 | 946.12 | 950.07 |
| 90 | 933.29 | 933.30 | 937.66 | 941.89 | 945.98 | 949.94 |
| 100 | 933.04 | 933.05 | 937.43 | 941.68 | 945.79 | 949.76 |
| 110 | 932.72 | 932.73 | 937.13 | 941.40 | 945.53 | 949.53 |
| 120 | 932.32 | 932.33 | 936.76 | 941.06 | 945.22 | 949.24 |
| 130 | 931.83 | 931.84 | 936.31 | 940.64 | 944.83 | 948.89 |
| 140 | 931.26 | 931.27 | 935.77 | 940.14 | 944.37 | 948.48 |
| 150 | 930.61 | 930.61 | 935.16 | 939.57 | 943.85 | 948.00 |
| 160 | 929.86 | 929.87 | 934.46 | 938.93 | 943.25 | 947.45 |
| 170 | 929.04 | 929.05 | 933.69 | 938.21 | 942.59 | 946.84 |
| 180 | 928.14 | 928.15 | 932.85 | 937.42 | 941.86 | 946.17 |
| 190 | 927.17 | 927.18 | 931.93 | 936.56 | 941.06 | 945.44 |
| 200 | 926.12 | 926.13 | 930.95 | 935.64 | 940.21 | 944.65 |
| 210 | 925.01 | 925.02 | 929.90 | 934.66 | 939.30 | 943.81 |
| 220 | 923.84 | 923.85 | 928.80 | 933.63 | 938.33 | 942.91 |
| 230 | 922.61 | 922.62 | 927.63 | 932.53 | 937.31 | 941.97 |
| 240 | 921.32 | 921.33 | 926.42 | 931.39 | 936.24 | 940.98 |
| 250 | 919.99 | 920.00 | 925.15 | 930.20 | 935.12 | 939.94 |
| 260 | 918.60 | 918.61 | 923.84 | 928.96 | — | — |
| 270 | 917.17 | 917.18 | — | — | — | — |
| 273 | 916.73 | 916.74 | — | — | — | — |

used for all computations in this Appendix. A list of properties at the triple point and at the normal pressure melting point is given in Table 18. Properties along the melting curve are reported in Table 19, along the sublimation curve in Table 20.

The exact locations of possible phase transition lines between ice Ih and ices II, III, IX, or XI are still relatively uncertain [see e.g. Lobban *et al.* (1998)] and not considered in the graphs and tables below.

In the following tables, figures are reported with several digits, not strictly dependent on the experimental uncertainty of the particular quantity. In many cases, as for several properties at higher pressures, this uncertainty is simply unknown. Sometimes, differences between given figures may have smaller uncertainties than the reported absolute values themselves. Summaries of uncertainties are provided in Tables 5 and 7. The many digits given in Table 18 are intended for use as numerical check values.
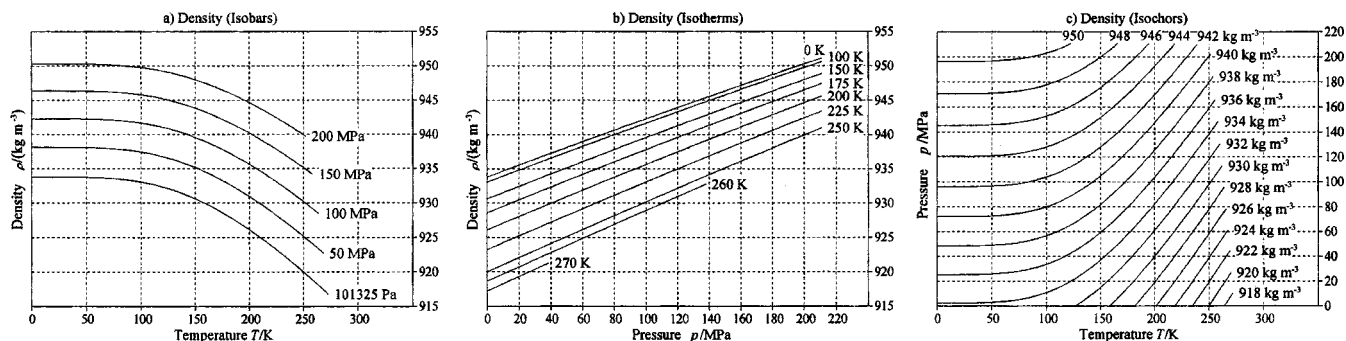


FIG. 10. Density $\rho(T,p)$ in kg m$^{-3}$ as a function of temperature for several pressures as indicated at the isobars in panel (a), as a function of pressure for several temperatures as indicated at the isotherms, panel (b), and isochors as functions of pressure and temperature, belonging to densities as indicated at the curves, panel (c). Values were computed from Eq. (4).

TABLE 12. Specific entropy, $s(T,p)$, Eq. (5), in J kg$^{-1}$ K$^{-1}$

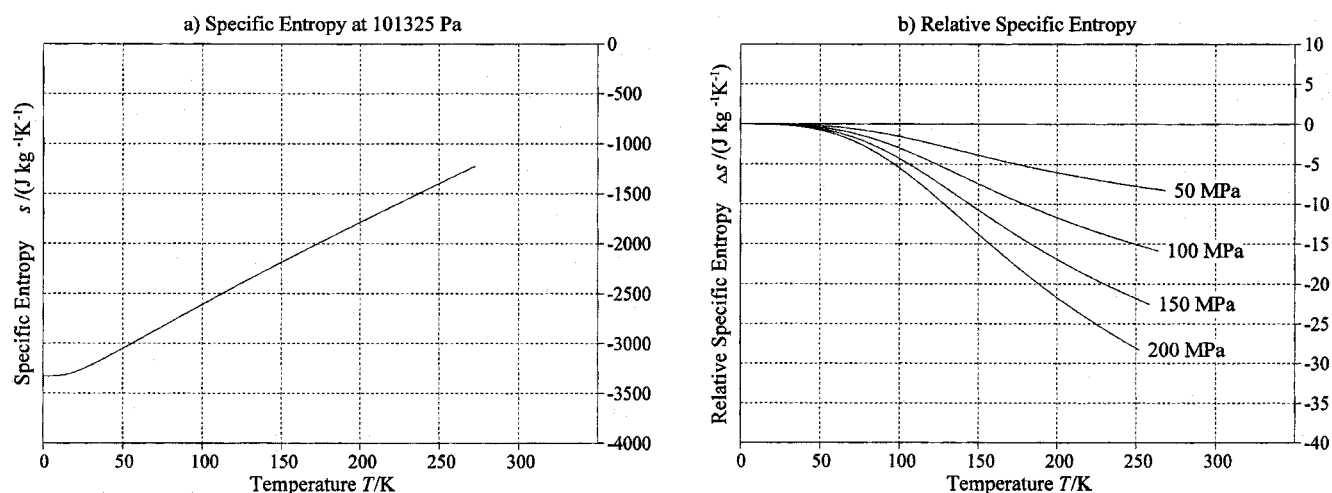| Temp. (K) | Pressure | | | | | |
|---|---|---|---|---|---|---|
| | 0 Pa | 101 325 Pa | 50 MPa | 100 MPa | 150 MPa | 200 MPa |
| 0 | −3327.34 | −3327.34 | −3327.34 | −3327.34 | −3327.34 | −3327.34 |
| 10 | −3323.00 | −3323.00 | −3323.00 | −3323.01 | −3323.01 | −3323.01 |
| 20 | −3287.38 | −3287.38 | −3287.39 | −3287.41 | −3287.42 | −3287.43 |
| 30 | −3219.29 | −3219.29 | −3219.34 | −3219.38 | −3219.42 | −3219.46 |
| 40 | −3138.01 | −3138.01 | −3138.12 | −3138.22 | −3138.31 | −3138.39 |
| 50 | −3051.81 | −3051.81 | −3052.02 | −3052.22 | −3052.39 | −3052.55 |
| 60 | −2963.58 | −2963.58 | −2963.95 | −2964.29 | −2964.59 | −2964.87 |
| 70 | −2874.58 | −2874.58 | −2875.16 | −2875.69 | −2876.17 | −2876.60 |
| 80 | −2785.50 | −2785.51 | −2786.35 | −2787.13 | −2787.84 | −2788.48 |
| 90 | −2696.84 | −2696.85 | −2698.02 | −2699.11 | −2700.09 | −2700.98 |
| 100 | −2608.95 | −2608.96 | −2610.52 | −2611.95 | −2613.26 | −2614.44 |
| 110 | −2522.08 | −2522.08 | −2524.07 | −2525.90 | −2527.57 | −2529.08 |
| 120 | −2436.37 | −2436.37 | −2438.81 | −2441.07 | −2443.13 | −2444.99 |
| 130 | −2351.86 | −2351.87 | −2354.78 | −2357.48 | −2359.95 | −2362.19 |
| 140 | −2268.53 | −2268.53 | −2271.93 | −2275.08 | −2277.96 | −2280.58 |
| 150 | −2186.28 | −2186.28 | −2190.17 | −2193.76 | −2197.06 | −2200.06 |
| 160 | −2104.99 | −2105.00 | −2109.35 | −2113.39 | −2117.09 | −2120.47 |
| 170 | −2024.54 | −2024.55 | −2029.36 | −2033.82 | −2037.93 | −2041.68 |
| 180 | −1944.81 | −1944.82 | −1950.06 | −1954.93 | −1959.42 | −1963.53 |
| 190 | −1865.67 | −1865.68 | −1871.34 | −1876.61 | −1881.47 | −1885.92 |
| 200 | −1787.03 | −1787.04 | −1793.10 | −1798.74 | −1803.96 | −1808.74 |
| 210 | −1708.81 | −1708.82 | −1715.26 | −1721.26 | −1726.81 | −1731.91 |
| 220 | −1630.93 | −1630.94 | −1637.74 | −1644.08 | −1649.95 | −1655.36 |
| 230 | −1553.33 | −1553.34 | −1560.48 | −1567.15 | −1573.34 | −1579.04 |
| 240 | −1475.97 | −1475.99 | −1483.45 | −1490.43 | −1496.91 | −1502.89 |
| 250 | −1398.81 | −1398.83 | −1406.60 | −1413.87 | −1420.64 | −1426.89 |
| 260 | −1321.81 | −1321.83 | −1329.90 | −1337.46 | — | — |
| 270 | −1244.96 | −1244.97 | — | — | — | — |
| 273 | −1221.92 | −1221.94 | — | — | — | — |



FIG. 11. Specific entropy $s(T,p_0)$ in J kg$^{-1}$ K$^{-1}$ at normal pressure, panel (a), and relative to normal pressure, $\Delta s = s(T,p) - s(T,p_0)$, panel (b), for several pressures $p$ as indicated at the curves. Values were computed from Eq. (5).

TABLE 13. Specific isobaric heat capacity, $c_p(T,p)$, Eq. (6), in $J\,kg^{-1}\,K^{-1}$

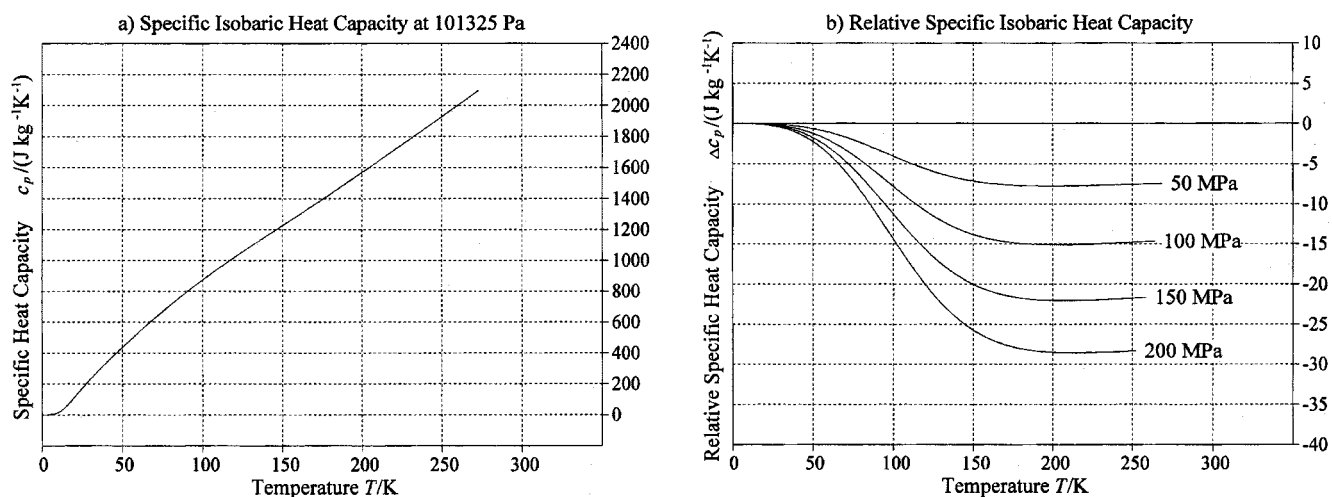| Temp. (K) | Pressure | | | | | |
|---|---|---|---|---|---|---|
| | 0 Pa | 101 325 Pa | 50 MPa | 100 MPa | 150 MPa | 200 MPa |
| 0 | 0.00 | 0.00 | 0.00 | 0.00 | 0.00 | 0.00 |
| 10 | 14.80 | 14.80 | 14.79 | 14.79 | 14.79 | 14.78 |
| 20 | 111.43 | 111.43 | 111.39 | 111.35 | 111.32 | 111.29 |
| 30 | 230.66 | 230.66 | 230.52 | 230.4 | 230.28 | 230.18 |
| 40 | 337.89 | 337.89 | 337.56 | 337.26 | 336.98 | 336.74 |
| 50 | 437.49 | 437.49 | 436.85 | 436.27 | 435.73 | 435.26 |
| 60 | 532.56 | 532.56 | 531.47 | 530.47 | 529.56 | 528.74 |
| 70 | 623.92 | 623.92 | 622.24 | 620.69 | 619.28 | 618.02 |
| 80 | 711.48 | 711.48 | 709.08 | 706.87 | 704.85 | 703.03 |
| 90 | 794.94 | 794.93 | 791.72 | 788.75 | 786.05 | 783.59 |
| 100 | 874.15 | 874.14 | 870.08 | 866.33 | 862.90 | 859.78 |
| 110 | 949.39 | 949.38 | 944.50 | 939.98 | 935.83 | 932.05 |
| 120 | 1021.31 | 1021.30 | 1015.68 | 1010.46 | 1005.65 | 1001.26 |
| 130 | 1090.81 | 1090.80 | 1084.55 | 1078.73 | 1073.35 | 1068.43 |
| 140 | 1158.84 | 1158.82 | 1152.06 | 1145.76 | 1139.92 | 1134.56 |
| 150 | 1226.20 | 1226.18 | 1219.04 | 1212.37 | 1206.17 | 1200.45 |
| 160 | 1293.52 | 1293.51 | 1286.10 | 1279.15 | 1272.69 | 1266.70 |
| 170 | 1361.23 | 1361.21 | 1353.62 | 1346.49 | 1339.83 | 1333.65 |
| 180 | 1429.54 | 1429.53 | 1421.84 | 1414.59 | 1407.80 | 1401.47 |
| 190 | 1498.58 | 1498.57 | 1490.83 | 1483.51 | 1476.63 | 1470.20 |
| 200 | 1568.37 | 1568.35 | 1560.60 | 1553.25 | 1546.33 | 1539.83 |
| 210 | 1638.88 | 1638.86 | 1631.12 | 1623.77 | 1616.82 | 1610.27 |
| 220 | 1710.04 | 1710.03 | 1702.33 | 1694.99 | 1688.03 | 1681.45 |
| 230 | 1781.81 | 1781.79 | 1774.13 | 1766.82 | 1759.86 | 1753.26 |
| 240 | 1854.09 | 1854.08 | 1846.48 | 1839.19 | 1832.24 | 1825.63 |
| 250 | 1926.85 | 1926.83 | 1919.28 | 1912.03 | 1905.09 | 1898.46 |
| 260 | 2000.00 | 1999.98 | 1992.49 | 1985.27 | — | — |
| 270 | 2073.49 | 2073.48 | — | — | — | — |
| 273 | 2095.60 | 2095.59 | — | — | — | — |



FIG. 12. Specific isobaric heat capacity $c_p(T,p_0)$ in $J\,kg^{-1}\,K^{-1}$ at normal pressure, panel (a), and relative to normal pressure, $\Delta c_p = c_p(T,p) - c_p(T,p_0)$, panel (b), for several pressures $p$ as indicated at the curves. Values were computed from Eq. (6).

TABLE 14. Specific enthalpy, $h(T,p)$, Eq. (7), in kJ kg$^{-1}$

| Temp. (K) | Pressure | | | | | |
|---|---|---|---|---|---|---|
| | 0 Pa | 101 325 Pa | 50 MPa | 100 MPa | 150 MPa | 200 MPa |
| 0 | −632.129 | −632.020 | −578.708 | −525.530 | −472.583 | −419.860 |
| 10 | −632.095 | −631.987 | −578.675 | −525.496 | −472.550 | −419.826 |
| 20 | −631.526 | −631.417 | −578.105 | −524.927 | −471.981 | −419.257 |
| 30 | −629.806 | −629.698 | −576.387 | −523.209 | −470.264 | −417.541 |
| 40 | −626.955 | −626.846 | −573.538 | −520.362 | −467.419 | −414.697 |
| 50 | −623.073 | −622.965 | −569.661 | −516.490 | −463.550 | −410.832 |
| 60 | −618.220 | −618.111 | −564.816 | −511.653 | −458.720 | −406.009 |
| 70 | −612.434 | −612.326 | −559.044 | −505.894 | −452.973 | −400.271 |
| 80 | −605.754 | −605.646 | −552.384 | −499.252 | −446.348 | −393.663 |
| 90 | −598.219 | −598.110 | −544.877 | −491.771 | −438.890 | −386.226 |
| 100 | −589.870 | −589.761 | −536.564 | −483.492 | −430.642 | −378.005 |
| 110 | −580.749 | −580.641 | −527.488 | −474.457 | −421.645 | −369.043 |
| 120 | −570.893 | −570.785 | −517.685 | −464.703 | −411.936 | −359.375 |
| 130 | −560.331 | −560.223 | −507.182 | −454.255 | −401.539 | −349.025 |
| 140 | −549.082 | −548.974 | −495.998 | −443.132 | −390.472 | −338.009 |
| 150 | −537.156 | −537.048 | −484.143 | −431.341 | −378.742 | −326.334 |
| 160 | −524.558 | −524.450 | −471.617 | −418.884 | −366.348 | −313.999 |
| 170 | −511.284 | −511.177 | −458.419 | −405.757 | −353.286 | −300.998 |
| 180 | −497.331 | −497.224 | −444.543 | −391.952 | −339.549 | −287.323 |
| 190 | −482.691 | −482.584 | −429.980 | −377.462 | −325.127 | −272.966 |
| 200 | −467.357 | −467.250 | −414.723 | −362.279 | −310.013 | −257.916 |
| 210 | −451.321 | −451.215 | −398.765 | −346.394 | −294.198 | −242.166 |
| 220 | −434.577 | −434.471 | −382.099 | −329.801 | −277.674 | −225.708 |
| 230 | −417.118 | −417.012 | −364.717 | −312.493 | −260.435 | −208.535 |
| 240 | −398.939 | −398.833 | −346.614 | −294.463 | −242.475 | −190.641 |
| 250 | −380.035 | −379.929 | −327.786 | −275.707 | −223.789 | −172.021 |
| 260 | −360.401 | −360.295 | −308.227 | −256.221 | — | — |
| 270 | −340.034 | −339.928 | — | — | — | — |
| 273 | −333.780 | −333.675 | — | — | — | — |

TABLE 15. Cubic expansion coefficient, $\alpha(T,p)$, Eq. (10), in $10^{-6}$ K$^{-1}$

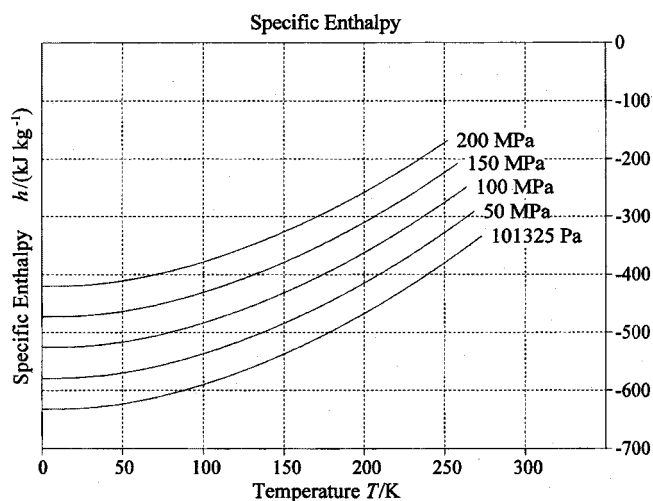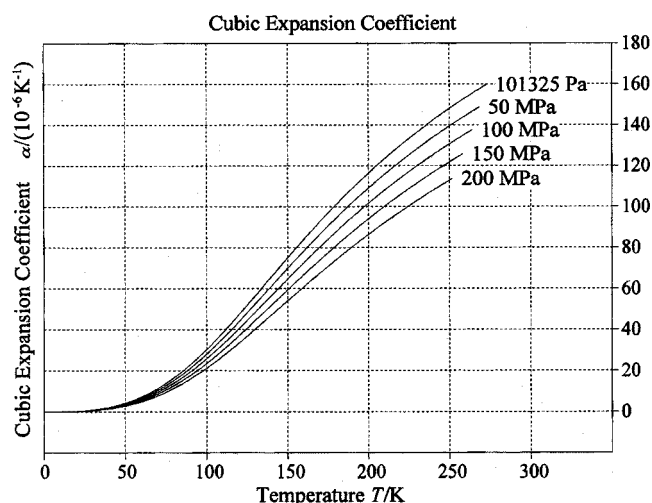| Temp. (K) | Pressure | | | | | |
|---|---|---|---|---|---|---|
| | 0 Pa | 101 325 Pa | 50 MPa | 100 MPa | 150 MPa | 200 MPa |
| 0 | 0.00 | 0.00 | 0.00 | 0.00 | 0.00 | 0.00 |
| 10 | 0.03 | 0.03 | 0.03 | 0.03 | 0.03 | 0.02 |
| 20 | 0.27 | 0.27 | 0.25 | 0.23 | 0.20 | 0.18 |
| 30 | 0.91 | 0.91 | 0.83 | 0.76 | 0.69 | 0.62 |
| 40 | 2.15 | 2.15 | 1.98 | 1.81 | 1.64 | 1.46 |
| 50 | 4.19 | 4.18 | 3.86 | 3.53 | 3.20 | 2.86 |
| 60 | 7.19 | 7.19 | 6.64 | 6.07 | 5.51 | 4.93 |
| 70 | 11.29 | 11.29 | 10.43 | 9.55 | 8.67 | 7.78 |
| 80 | 16.55 | 16.55 | 15.30 | 14.03 | 12.75 | 11.46 |
| 90 | 22.94 | 22.94 | 21.23 | 19.49 | 17.74 | 15.96 |
| 100 | 30.36 | 30.36 | 28.12 | 25.85 | 23.56 | 21.24 |
| 110 | 38.61 | 38.61 | 35.80 | 32.95 | 30.07 | 27.16 |
| 120 | 47.46 | 47.45 | 44.05 | 40.60 | 37.11 | 33.58 |
| 130 | 56.64 | 56.63 | 52.63 | 48.57 | 44.47 | 40.32 |
| 140 | 65.93 | 65.93 | 61.34 | 56.68 | 51.98 | 47.22 |
| 150 | 75.15 | 75.14 | 69.99 | 64.76 | 59.48 | 54.14 |
| 160 | 84.13 | 84.12 | 78.45 | 72.69 | 66.87 | 60.98 |
| 170 | 92.80 | 92.79 | 86.63 | 80.38 | 74.05 | 67.66 |
| 180 | 101.08 | 101.07 | 94.47 | 87.77 | 80.99 | 74.13 |
| 190 | 108.96 | 108.95 | 101.95 | 94.84 | 87.65 | 80.37 |
| 200 | 116.42 | 116.41 | 109.05 | 101.58 | 94.02 | 86.36 |
| 210 | 123.48 | 123.46 | 115.78 | 107.99 | 100.10 | 92.11 |
| 220 | 130.14 | 130.12 | 122.16 | 114.08 | 105.90 | 97.61 |
| 230 | 136.43 | 136.41 | 128.21 | 119.87 | 111.43 | 102.88 |
| 240 | 142.37 | 142.35 | 133.93 | 125.37 | 116.70 | 107.93 |
| 250 | 147.98 | 147.96 | 139.36 | 130.61 | 121.75 | 112.77 |
| 260 | 153.29 | 153.28 | 144.51 | 135.60 | — | — |
| 270 | 158.33 | 158.31 | — | — | — | — |
| 273 | 159.79 | 159.77 | — | — | — | — |



FIG. 13. Specific enthalpy $h(T,p)$ in kJ kg$^{-1}$ as a function of temperature for several pressures as indicated at the curves. Values were computed from Eq. (7).



FIG. 14. Cubic expansion coefficient $\alpha(T,p)$ in $10^{-6}$ K$^{-1}$ for several pressures as indicated at the curves. Values were computed from Eq. (10).

TABLE 16. Pressure coefficient, $\beta(T,p)$, Eq. (11), in kPa K$^{-1}$

| Temp. (K) | Pressure | | | | | |
|---|---|---|---|---|---|---|
| | 0 Pa | 101 325 Pa | 50 MPa | 100 MPa | 150 MPa | 200 MPa |
| 0 | 0.0 | 0.0 | 0.0 | 0.0 | 0.0 | 0.0 |
| 10 | 0.4 | 0.4 | 0.3 | 0.3 | 0.3 | 0.3 |
| 20 | 2.8 | 2.8 | 2.7 | 2.6 | 2.4 | 2.2 |
| 30 | 9.6 | 9.6 | 9.2 | 8.7 | 8.2 | 7.6 |
| 40 | 22.7 | 22.7 | 21.8 | 20.7 | 19.4 | 18.0 |
| 50 | 44.2 | 44.2 | 42.4 | 40.3 | 38.0 | 35.3 |
| 60 | 75.9 | 75.9 | 72.8 | 69.3 | 65.3 | 60.7 |
| 70 | 119.0 | 119.0 | 114.3 | 108.8 | 102.6 | 95.6 |
| 80 | 174.1 | 174.1 | 167.3 | 159.4 | 150.5 | 140.3 |
| 90 | 240.6 | 240.6 | 231.4 | 220.8 | 208.6 | 194.8 |
| 100 | 317.1 | 317.1 | 305.2 | 291.5 | 275.7 | 257.9 |
| 110 | 401.2 | 401.2 | 386.4 | 369.4 | 349.9 | 327.8 |
| 120 | 489.9 | 489.9 | 472.3 | 451.9 | 428.6 | 402.1 |
| 130 | 580.3 | 580.3 | 559.8 | 536.2 | 509.1 | 478.3 |
| 140 | 669.7 | 669.6 | 646.5 | 619.7 | 589.1 | 554.3 |
| 150 | 755.8 | 755.8 | 730.1 | 700.5 | 666.5 | 628.1 |
| 160 | 837.1 | 837.1 | 809.2 | 776.9 | 740.0 | 698.3 |
| 170 | 912.6 | 912.6 | 882.7 | 848.1 | 808.6 | 763.9 |
| 180 | 981.8 | 981.8 | 950.1 | 913.5 | 871.8 | 824.6 |
| 190 | 1044.6 | 1044.6 | 1011.3 | 973.0 | 929.4 | 880.1 |
| 200 | 1101.1 | 1101.0 | 1066.5 | 1026.7 | 981.5 | 930.4 |
| 210 | 1151.5 | 1151.4 | 1115.8 | 1074.8 | 1028.3 | 975.7 |
| 220 | 1196.2 | 1196.2 | 1159.6 | 1117.7 | 1070.0 | 1016.4 |
| 230 | 1235.8 | 1235.7 | 1198.4 | 1155.7 | 1107.2 | 1052.7 |
| 240 | 1270.5 | 1270.4 | 1232.6 | 1189.2 | 1140.1 | 1085.0 |
| 250 | 1301.0 | 1300.9 | 1262.6 | 1218.8 | 1169.2 | 1113.6 |
| 260 | 1327.5 | 1327.4 | 1288.8 | 1244.7 | — | — |
| 270 | 1350.5 | 1350.5 | — | — | — | — |
| 273 | 1356.8 | 1356.7 | — | — | — | — |

TABLE 17. Isothermal compressibility, $\kappa_T(T,p)$, Eq. (12), in TPa$^{-1}$

| Temp. (K) | Pressure | | | | | |
|---|---|---|---|---|---|---|
| | 0 Pa | 101 325 Pa | 50 MPa | 100 MPa | 150 MPa | 200 MPa |
| 0 | 94.54 | 94.53 | 90.91 | 87.46 | 84.18 | 81.09 |
| 10 | 94.54 | 94.53 | 90.91 | 87.46 | 84.18 | 81.09 |
| 20 | 94.54 | 94.53 | 90.91 | 87.46 | 84.18 | 81.09 |
| 30 | 94.55 | 94.54 | 90.92 | 87.47 | 84.19 | 81.10 |
| 40 | 94.57 | 94.57 | 90.95 | 87.49 | 84.22 | 81.13 |
| 50 | 94.62 | 94.61 | 90.99 | 87.54 | 84.27 | 81.18 |
| 60 | 94.71 | 94.70 | 91.08 | 87.63 | 84.36 | 81.27 |
| 70 | 94.85 | 94.84 | 91.22 | 87.77 | 84.50 | 81.41 |
| 80 | 95.06 | 95.05 | 91.43 | 87.99 | 84.72 | 81.63 |
| 90 | 95.35 | 95.34 | 91.73 | 88.29 | 85.02 | 81.94 |
| 100 | 95.74 | 95.73 | 92.13 | 88.69 | 85.43 | 82.35 |
| 110 | 96.24 | 96.24 | 92.64 | 89.20 | 85.95 | 82.87 |
| 120 | 96.86 | 96.85 | 93.26 | 89.83 | 86.59 | 83.52 |
| 130 | 97.60 | 97.59 | 94.01 | 90.59 | 87.35 | 84.29 |
| 140 | 98.46 | 98.45 | 94.88 | 91.47 | 88.24 | 85.19 |
| 150 | 99.43 | 99.42 | 95.86 | 92.46 | 89.24 | 86.20 |
| 160 | 100.50 | 100.50 | 96.95 | 93.57 | 90.36 | 87.33 |
| 170 | 101.68 | 101.67 | 98.14 | 94.77 | 91.58 | 88.57 |
| 180 | 102.95 | 102.95 | 99.43 | 96.08 | 92.90 | 89.90 |
| 190 | 104.31 | 104.30 | 100.80 | 97.47 | 94.31 | 91.32 |
| 200 | 105.74 | 105.73 | 102.25 | 98.93 | 95.79 | 92.82 |
| 210 | 107.23 | 107.23 | 103.77 | 100.47 | 97.35 | 94.40 |
| 220 | 108.79 | 108.78 | 105.35 | 102.07 | 98.96 | 96.04 |
| 230 | 110.40 | 110.39 | 106.98 | 103.72 | 100.64 | 97.73 |
| 240 | 112.05 | 112.05 | 108.66 | 105.42 | 102.36 | 99.47 |
| 250 | 113.75 | 113.74 | 110.38 | 107.17 | 104.13 | 101.26 |
| 260 | 115.48 | 115.47 | 112.13 | 108.94 | — | — |
| 270 | 117.23 | 117.23 | — | — | — | — |
| 273 | 117.77 | 117.76 | — | — | — | — |
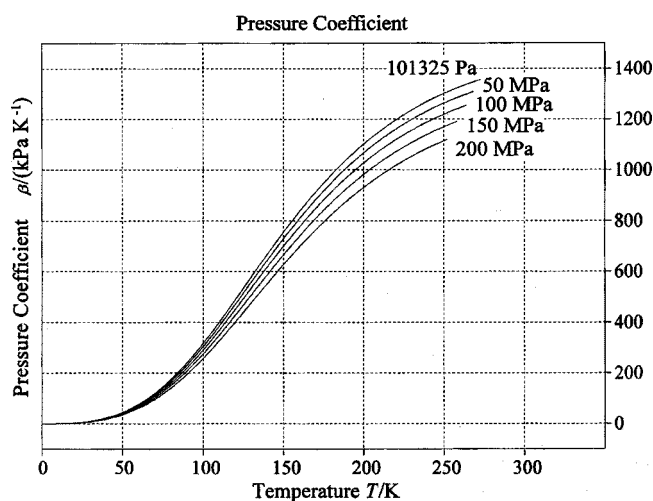


FIG. 15. Pressure coefficient $\beta(T,p)$ in kPa K$^{-1}$ for several pressures as indicated at the curves. Values were computed from Eq. (11).
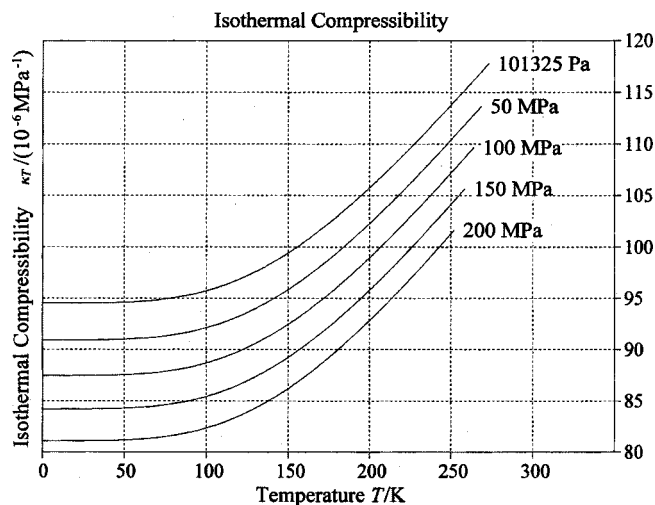


FIG. 16. Isothermal compressibility $\kappa_T(T,p)$ in $10^6$ MPa$^{-1}$ for several pressures as indicated at the curves. Values were computed from Eq. (12).

TABLE 18. Properties at the triple point and the normal pressure melting point, usable as numerical check values. The numerical functions evaluated here at given points $(T,p)$ are defined in Eq. (1) and Tables 3 and 4

| Quantity | Value at $T_t$, $p_t$ | Value at $T_{\text{melt},p_0}$, $p_0$ | Unit |
|---|---|---|---|
| $p$ | 611.657 | 101 325 | Pa |
| $T$ | 273.16 | 273.152 519 | K |
| $g$ | 0.611 670 524 | 101.342 627 076 | J kg$^{-1}$ |
| $(\partial g/\partial p)_T$ | 1.090 858 127 366 4E−03 | 1.090 843 882 143 11E−03 | m$^3$ kg$^{-1}$ |
| $(\partial g/\partial T)_p$ | 1220.694 339 396 87 | 1220.769 325 496 96 | J kg$^{-1}$ K$^{-1}$ |
| $(\partial^2 g/\partial p^2)_T$ | −1.284 959 415 714 94E−13 | −1.284 853 649 284 55E−13 | m$^3$ kg$^{-1}$ Pa$^{-1}$ |
| $\partial^2 g/\partial p\partial T$ | 1.743 879 646 995 98E−07 | 1.743 622 199 721 59E−07 | m$^3$ kg$^{-1}$ K$^{-1}$ |
| $(\partial^2 g/\partial T^2)_p$ | −7.676 029 858 750 67 | −7.675 982 333 647 98 | J kg$^{-1}$ K$^{-2}$ |
| $h$ | −333 444.254 079 125 | −333 354.873 750 348 | J kg$^{-1}$ |
| $f$ | −0.055 560 486 077 8842 | −9.187 129 281 834 95 | J kg$^{-1}$ |
| $u$ | −333 444.921 310 135 | −333 465.403 506 706 | J kg$^{-1}$ |
| $c_p$ | 2 096.784 316 216 33 | 2 096.713 910 235 44 | J kg$^{-1}$ K$^{-1}$ |
| $\rho$ | 916.709 492 199 729 | 916.721 463 419 096 | kg m$^{-3}$ |
| $\alpha$ | 1.598 631 025 655 13E−04 | 1.598 415 894 578 8E−04 | K$^{-1}$ |
| $\beta$ | 1357 147.646 585 94 | 1 357 058.993 211 01 | Pa K$^{-1}$ |
| $\kappa_T$ | 1.177 934 493 477 31E−10 | 1.177 852 917 651 5E−10 | Pa$^{-1}$ |
| $\kappa_s$ | 1.141 615 977 786 3E−10 | 1.141 544 425 564 98E−10 | Pa$^{-1}$ |

TABLE 19. Properties on the melting curve. Differences of specific volumes and enthalpies between liquid water and ice are defined as $\Delta\nu_{\text{melt}}=\nu^L-\nu$ and $\Delta h_{\text{melt}}=h^L-h$. The corresponding differences are $\Delta g=g^L-g=0$ in specific Gibbs energy and therefore $\Delta s_{\text{melt}}=s^L-s=\Delta h_{\text{melt}}/T$ in specific entropy

| $T$ (K) | $p$ (MPa) | $\nu$ (cm$^3$ kg$^{-1}$) | $\Delta\nu_{\text{melt}}$ (cm$^3$ kg$^{-1}$) | $h$ (kJ kg$^{-1}$) | $\Delta h_{\text{melt}}$ (kJ kg$^{-1}$) | $g$ (kJ kg$^{-1}$) | $s$ (J kg$^{-1}$ K$^{-1}$) |
|---|---|---|---|---|---|---|---|
| 273.16 | 0.0006 | 1090.86 | −90.65 | −333.444 | 333.446 | 0.001 | −1220.69 |
| 273.152519 | 0.1013 | 1090.84 | −90.69 | −333.355 | 333.427 | 0.101 | −1220.77 |
| 273 | 2.1453 | 1090.55 | −91.43 | −331.542 | 333.051 | 2.144 | −1222.30 |
| 272 | 15.1355 | 1088.73 | −96.01 | −320.088 | 330.518 | 15.072 | −1232.20 |
| 271 | 27.4942 | 1087.00 | −100.19 | −309.291 | 327.883 | 27.279 | −1241.96 |
| 270 | 39.3133 | 1085.35 | −104.05 | −299.056 | 325.167 | 38.870 | −1251.58 |
| 269 | 50.6633 | 1083.78 | −107.63 | −289.307 | 322.385 | 49.924 | −1261.08 |
| 268 | 61.5996 | 1082.28 | −110.97 | −279.986 | 319.551 | 60.502 | −1270.48 |
| 267 | 72.1668 | 1080.84 | −114.09 | −271.046 | 316.677 | 70.656 | −1279.78 |
| 266 | 82.4018 | 1079.45 | −117.03 | −262.448 | 313.770 | 80.427 | −1289.00 |
| 265 | 92.3352 | 1078.12 | −119.80 | −254.159 | 310.842 | 89.849 | −1298.15 |
| 264 | 101.9928 | 1076.82 | −122.41 | −246.153 | 307.898 | 98.953 | −1307.22 |
| 263 | 111.3970 | 1075.57 | −124.89 | −238.405 | 304.947 | 107.761 | −1316.22 |
| 262 | 120.5669 | 1074.36 | −127.24 | −230.896 | 301.995 | 116.298 | −1325.17 |
| 261 | 129.5195 | 1073.18 | −129.48 | −223.607 | 299.049 | 124.582 | −1334.05 |
| 260 | 138.2699 | 1072.04 | −131.61 | −216.522 | 296.116 | 132.629 | −1342.89 |
| 259 | 146.8313 | 1070.93 | −133.64 | −209.629 | 293.201 | 140.455 | −1351.67 |
| 258 | 155.2158 | 1069.85 | −135.57 | −202.913 | 290.313 | 148.074 | −1360.41 |
| 257 | 163.4344 | 1068.79 | −137.42 | −196.363 | 287.456 | 155.497 | −1369.11 |
| 256 | 171.4972 | 1067.76 | −139.19 | −189.969 | 284.637 | 162.737 | −1377.76 |
| 255 | 179.4135 | 1066.76 | −140.88 | −183.721 | 281.864 | 169.804 | −1386.37 |
| 254 | 187.1919 | 1065.78 | −142.50 | −177.609 | 279.142 | 176.707 | −1394.95 |
| 253 | 194.8407 | 1064.82 | −144.04 | −171.626 | 276.479 | 183.456 | −1403.49 |
| 252 | 202.3675 | 1063.89 | −145.53 | −165.763 | 273.882 | 190.059 | −1411.99 |
| 251 | 209.7797 | 1062.97 | −146.94 | −160.012 | 271.358 | 196.526 | −1420.47 |
| 250 | 217.0846 | 1062.07 | −148.30 | −154.366 | 268.915 | 202.862 | −1428.91 |

TABLE 20. Properties on the sublimation curve. Differences of specific volumes and enthalpies between water vapor and ice are defined as $\Delta\nu_{subl} = \nu^V - \nu$ and $\Delta h_{subl} = h^V - h$. The corresponding differences are $\Delta g = g^V - g = 0$ in specific Gibbs energy and therefore $\Delta s_{subl} = s^V - s = \Delta h_{subl}/T$ in specific entropy

| $T$ (K) | $p$ (Pa) | $\nu$ (cm$^3$ kg$^{-1}$) | $\Delta\nu_{subl}$ (cm$^3$ kg$^{-1}$) | $h$ (kJ kg$^{-1}$) | $\Delta h_{subl}$ (kJ kg$^{-1}$) | $g$ (kJ kg$^{-1}$) | $s$ (J kg$^{-1}$ K$^{-1}$) |
|---|---|---|---|---|---|---|---|
| 273.16 | 611.66 | 1090.86 | 2.0599E+08 | −333.444 | 2834.359 | +0.001 | −1220.69 |
| 270 | 470.06 | 1090.31 | 2.6497E+08 | −340.033 | 2835.166 | −3.895 | −1244.96 |
| 265 | 305.91 | 1089.45 | 3.9965E+08 | −350.309 | 2836.269 | −10.216 | −1283.37 |
| 260 | 195.80 | 1088.61 | 6.1267E+08 | −360.401 | 2837.165 | −16.729 | −1321.81 |
| 255 | 123.14 | 1087.79 | 9.5552E+08 | −370.309 | 2837.860 | −23.435 | −1360.29 |
| 250 | 76.016 | 1086.97 | 1.5176E+09 | −380.035 | 2838.358 | −30.332 | −1398.81 |
| 245 | 46.008 | 1086.18 | 2.4574E+09 | −389.578 | 2838.664 | −37.423 | −1437.37 |
| 240 | 27.269 | 1085.40 | 4.0617E+09 | −398.939 | 2838.781 | −44.706 | −1475.97 |
| 235 | 15.806 | 1084.63 | 6.8613E+09 | −408.119 | 2838.710 | −52.183 | −1514.62 |
| 230 | 8.9479 | 1083.88 | 1.1863E+10 | −417.118 | 2838.456 | −59.853 | −1553.33 |
| 225 | 4.9393 | 1083.15 | 2.1023E+10 | −425.938 | 2838.020 | −67.716 | −1592.10 |
| 220 | 2.6542 | 1082.44 | 3.8254E+10 | −434.577 | 2837.403 | −75.774 | −1630.93 |
| 215 | 1.3859 | 1081.74 | 7.1598E+10 | −443.038 | 2836.607 | −84.026 | −1669.83 |
| 210 | 7.0172E−01 | 1081.07 | 1.3811E+11 | −451.321 | 2835.633 | −92.472 | −1708.81 |
| 205 | 3.4381E−01 | 1080.41 | 2.7519E+11 | −459.427 | 2834.483 | −101.114 | −1747.87 |
| 200 | 1.6260E−01 | 1079.77 | 5.6769E+11 | −467.357 | 2833.157 | −109.951 | −1787.03 |
| 195 | 7.4028E−02 | 1079.15 | 1.2157E+12 | −475.111 | 2831.656 | −118.984 | −1826.29 |
| 190 | 3.2352E−02 | 1078.56 | 2.7104E+12 | −482.691 | 2829.982 | −128.214 | −1865.67 |
| 185 | 1.3527E−02 | 1077.98 | 6.3117E+12 | −490.097 | 2828.135 | −137.641 | −1905.17 |
| 180 | 5.3921E−03 | 1077.42 | 1.5406E+13 | −497.331 | 2826.117 | −147.266 | −1944.81 |
| 175 | 2.0408E−03 | 1076.89 | 3.9576E+13 | −504.393 | 2823.927 | −157.089 | −1984.59 |
| 170 | 7.3007E−04 | 1076.38 | 1.0747E+14 | −511.284 | 2821.567 | −167.112 | −2024.54 |
| 165 | 2.4564E−04 | 1075.89 | 3.1001E+14 | −518.006 | 2819.038 | −177.335 | −2064.67 |
| 160 | 7.7289E−05 | 1075.43 | 9.5541E+14 | −524.558 | 2816.340 | −187.759 | −2104.99 |
| 155 | 2.2598E−05 | 1074.99 | 3.1655E+15 | −530.941 | 2813.474 | −198.385 | −2145.52 |
| 150 | 6.0957E−06 | 1074.57 | 1.1357E+16 | −537.156 | 2810.441 | −209.215 | −2186.28 |
| 145 | 1.5045E−06 | 1074.18 | 4.4479E+16 | −543.203 | 2807.239 | −220.249 | −2227.27 |
| 140 | 3.3662E−07 | 1073.81 | 1.9194E+17 | −549.082 | 2803.870 | −231.488 | −2268.53 |
| 135 | 6.7542E−08 | 1073.47 | 9.2246E+17 | −554.791 | 2800.332 | −242.934 | −2310.05 |
| 130 | 1.2004E−08 | 1073.15 | 4.9982E+18 | −560.331 | 2796.624 | −254.589 | −2351.86 |

# 8. References

Bramwell, S. T., Nature **397**, 212 (1999).

Bridgman, P. W., Proc. Am. Acad. Arts Sci. **47**, 441 (1912a).

Bridgman, P. W., Proc. Am. Acad. Arts Sci. **48**, 309 (1912b).

Bridgman, P. W., J. Chem. Phys. **3**, 597 (1935).

Bridgman, P. W., J. Chem. Phys. **5**, 964 (1937).

Brill, R. and A. Tippe, Acta Cryst. **23**, 343 (1967).

Brockamp, B. and H. Rüter, Z. Geophys. **35**, 277 (1969).

Bryson III, C. E., V. Cazcarra, and L. L. Levenson., J. Chem. Eng. Data **19**, 107 (1974).

Butkovich, T. R., J. Glaciol. **2**, 553 (1955).

Butkovich, T. R., SIPRE Res. Rep. **40**, 1 (1957).

Caldwell, D. R., Deep-Sea Res. **25**, 175 (1978).

Cox, J. D., D. D. Wagman, and V. A. Medvedev, *CODATA Key Values for Thermodynamics* (Hemisphere Publishing Corp., 1989).

Dantl, G., Z. Phys. **166**, 115 (1962); Berichtigung. Z. Phys. **169**, 466 (1962).

Dantl, G., *Elastische Moduln und mechanische Dämpfung in Eis-Einkristallen* (Dissertation, TH Stuttgart, 1967).

Dantl, G., Phys. Kondens. Materie **7**, 390 (1968).

Dantl, G., in *Physics of Ice*, edited by N. Riehl, B. Bullemer, and H. Engelhardt (Plenum, New York, 1969), p. 223.

Dantl, G. and I. Gregora, Naturwiss. **55**, 176 (1968).

Dengel, O., U. Eckener, H. Plitz, and N. Riehl, Phys. Lett. **9**, 291 (1964).

Dieterici, C., Ann. Physik **16**, 593 (1905).

Dorsey, N. E., *Properties of Ordinary Water-Substance* (Hafner Publishing Company, New York, 1968).

Douslin, D. R. and A. Osborn, J. Sci. Instrum. **42**, 369 (1965).

Feistel, R., Progr. Oceanogr. **58**, 43 (2003).

Feistel, R. and E. Hagen, Progr. Oceanogr. **36**, 249 (1995).

Feistel, R. and W. Wagner, J. Mar. Res. **63**, 95 (2005).

Feistel, R., W. Wagner, V. Tchijov, and C. Guder, Ocean Sci. Disc. **2**, 37 (2005); Ocean Sci. **1**, 29 (2005).

Fletcher, N. H., *The Chemical Physics of Ice* (Cambridge University Press, Cambridge, 1970).

Flubacher, P., A. J. Leadbetter, and J. A. Morrison, J. Chem. Phys. **33**, 1751 (1960).

Franks, F., in *Water—A Comprehensive Treatise*. Vol. 1. edited by F. Franks (Plenum, New York, London, 1972).

Fukusako, S., Int. J. Thermophys. **11**, 353 (1990).

Gagnon, R. E., H. Kiefte, M. J. Clouter, and E. Whalley, J. Chem. Phys. **89**, 4522 (1988).

Gammon, P. H., H. Kiefte, and M. J. Clouter, J. Glaciol. **25**, 159 (1980).

Gammon, P. H., H. Kiefte, M. J. Clouter, and W. W. Denner, J. Glaciol. **29**, 433 (1983).

Giauque, W. F. and J. W. Stout, J. Am. Chem. Soc. **58**, 1144 (1936).

Ginnings, D. C. and R. J. Corruccini, J. Res. Natl. Bur. Stand. **38**, 583 (1947).

Gordon, A. R., J. Chem. Phys. **2**, 65 (1934).

Griffiths, E., Proc. Phys. Soc. (London) **26**, 1 (1913).

Guildner, L. A., D. P. Johnson, and F. E. Jones, J. Res. Natl. Bur. Stand. **80A**, 505 (1976).

Haida, O., T. Matsuo, H. Suga, and S. Seki, J. Chem. Thermodyn. **6**, 815 (1974).

Henderson, S. J. and R. J. Speedy, J. Phys. Chem. **91**, 3096 (1987).

Hobbs, P. V., *Ice Physics* (Clarendon, Oxford, 1974).

Howe, R. and R. W. Whitworth, J. Chem. Phys. **90**, 4450 (1989).

Hyland, R. W. and A. Wexler, Trans. Am. Soc. Heat. Refrig. Air Cond. Eng. **89**, 500 (1983).

IAPWS, *Guideline on the Use of Fundamental Constants and Basic Con-*

*stants of Water* (The International Association for the Properties of Water and Steam, 2001, revision 2005).

Iedema, M. J., M. J. Dresser, D. L. Doering, J. B. Rowland, W. P. Hess, A. A. Tsekouras, and J. P. Cowin, J. Phys. Chem. B **102**, 9203 (1998).

ISO, *Guide to the Expression of Uncertainty in Measurement* (International Organization for Standardization, Geneva, 1993a).

ISO, *ISO Standards Handbook* (International Organization for Standardization, Geneva, 1993b).

Jakob, M. and S. Erk, Mitt. Phys.-Techn. Reichsanst. **35**, 302 (1929).

Jancso, G., J. Pupezin, and W. A. Van Hook, J. Phys. Chem. **74**, 2984 (1970).

Johari, G. P., J. Chem. Phys. **109**, 9543 (1998).

Johari, G. P. and S. J. Jones, J. Chem. Phys. **62**, 4213 (1975).

Kuo, J.-L., J. V. Coe, S. J. Singer, Y. B. Band, and L. Ojamäe, J. Chem. Phys. **114**, 2527 (2001).

Kuo, J.-L., M. L. Klein, S. J. Singer, and L. Ojamäe, in *Abstracts of Papers, 227th ACS National Meeting, Anaheim, CA, USA, March 28–April 1, 2004, PHYS-463* (American Chemical Society, 2004).

Landau, L. D. and E. M. Lifschitz, *Statistische Physik* (Akademie-Verlag, Berlin, 1966).

LaPlaca, S. and B. Post, Acta Cryst. **13**, 503 (1960).

Leadbetter, A. J., Proc. Roy. Soc. London **287**, 403 (1965).

Lobban, C., J. L. Finney, and W. F. Kuhs, Nature **391**, 268 (1998).

Lonsdale, D. K, Proc. Roy. Soc. London **247**, 424 (1958).

Marion, G. N. and S. D. Jakubowski, Cold Regions Sci. Technol. **38**, 211 (2004).

Marti, J. and K. Mauersberger, Geophys. Res. Lett. **20**, 363 (1993).

Matsuo, T., Y. Tajima, and H. Suga, J. Phys. Chem. Solids **47**, 165 (1986).

Mauersberger, K. and D. Krankowsky, Geophys. Res. Lett. **30**, 1121 (2003).

Megaw, H. D., Nature **134**, 900 (1934).

Millero, F. J., Unesco Techn. Pap. Mar. Sci. **28**, 29 (1978).

Mohr, P. J. and B. N. Taylor, Rev. Mod. Phys. **77**, 1 (2005).

Murphy, D. M. and T. Koop, Q. J. Royal Met. Society **608**, 1539 (2005).

Nagle, J. F., J. Math. Phys. **7**, 1484 (1966).

Nagornov, O. V. and V. E. Chizhov, J. Appl. Mech. Techn. Phys. **31**, 343 (1990).

NBS, *Announcement of Changes in Electrical and Photometric Units*, NBS Circular C459 (U.S. Government Printing Office, Washington, D.C., 1948).

Nicholas, J. V., T. D. Dransfield, and D. R. White, Metrologia **33**, 265 (1996).

Osborne, N. S., J. Res. Nat. Bur. Stand. **23**, 643 (1939).

Pauling, L., J. Amer. Chem. Soc. **57**, 2680 (1935).

Petrenko, V. F., CRREL Report **93–25**, 1 (1993).

Petrenko, V. F. and R. W. Whitworth, *Physics of Ice* (Oxford University Press, Oxford, 1999).

Pitzer, K. S. and J. Polissar, J. Phys. Chem. **60**, 1140 (1956).

Pounder, E. R., *Physics of Ice* (Pergamon, Oxford, 1965).

Preston-Thomas, H., Metrologia **27**, 3 (1990).

Proctor, T. M., Jr., J. Acoust. Soc. Amer. **39**, 972 (1966).

PTB, *Quecksilber. PTB-Stoffdatenblätter SDB 12* (Physikalisch-Technische Bundesanstalt, Braunschweig and Berlin, 1995).

Richards, T. W. and C. L. Speyers, J. Amer. Chem. Soc. **36**, 491 (1914).

Rossini, F. D., D. W. Wagman, W. H. Evans, S. Levine, and I. Jaffe, *Selected Values of Chemical Thermodynamic Properties*, Circular of the National Bureau of Standards 500 (US Government Printing Office, Washington, D.C., 1952).

Röttger, K., A. Endriss, J. Ihringer, S. Doyle, and W. F. Kuhs, Acta Crystall. **B50**, 644 (1994).

Singer, S. J., J.-L. Kuo, T. K. Hirsch, C. Knight, L. Ojamäe, and M. L. Klein, Phys. Rev. Lett. **94**, 135701 (2005).

Sugisaki, M., H. Suga, and S. Seki, Bull. Chem. Soc. Jpn. **41**, 2591 (1968).

Tanaka, H., J. Chem. Phys. **108**, 4887 (1998).

Tillner-Roth, R., *Fundamental Equations of State* (Shaker Verlag, Aachen, 1998).

Truby, F. K., Science **121**, 404 (1955).

van den Beukel, A., Phys. Status Solidi **28**, 565 (1968).

Wagner, W. and A. Pruß, J. Phys. Chem. Ref. Data **31**, 387 (2002).

Wagner, W., A. Saul, and A. Pruß, J. Phys. Chem. Ref. Data **23**, 515 (1994).

Wexler, A., J. Res. Nat. Bur. Stand. **81A**, 5 (1977).

White, D. R., T. D. Dransfield, G. F. Strouse, W. L. Tew, R. L. Rusby, and J. Gray, in *Temperature: Its Measurement and Control in Science and Industry*, Volume 7, *AIP Conference Proceedings 684*, edited by D.C. Ripple (American Institute of Physics, Melville, New York, 2003), p. 221.

Woolley, H. W., in *Water and Steam, Proceedings of the 9th International Conference on the Properties of Steam*, edited by J. Straub and K. Scheffler (Pergamon, New York, 1980), p. 166.

Yamamuro, O., M. Oguni, T. Matsuo, and H. Suga, J. Chem. Phys. **86**, 5137 (1987).

Yen, Y.-C., CCREL Report **81-10**, 1 (1981).

Yen, Y.-C., K. C. Cheng, and S. Fukusako, in *Proceedings 3rd International Symposium on Cold Regions Heat Transfer*, edited by J. P. Zarling and S. L. Faussett (Fairbanks, AL, 1991), p. 187.